

The 2-Channel Kondo Model I: Review of Experimental Evidence for its Realization in Metal Nanoconstrictions

Jan von Delft^{1,*}, D. C. Ralph¹, R. A. Buhrman², A. W. W. Ludwig³,
Vinay Ambegaokar¹

¹*Laboratory of Atomic and Solid State Physics, Cornell University, Ithaca, NY 14853, USA*

²*School of Applied and Engineering Physics, Cornell University, Ithaca, NY 14853, USA*

³*University of California, Santa Barbara, CA 93106, USA*

(February 4, 1997)

Abstract

Certain zero-bias anomalies (ZBAs) in the voltage, temperature and magnetic field dependence of the conductance $G(V, T, H)$ of quenched Cu point contacts have previously been interpreted to be due to non-magnetic 2-channel Kondo (2CK) scattering from near-degenerate atomic two-level tunneling systems^{1,2}, and hence to represent an experimental realization of the non-Fermi-liquid physics of the $T = 0$ fixed point of the 2-channel Kondo model. In this, the first in a series of three papers (I,II,III) devoted to 2-channel Kondo physics, we present a comprehensive review of the quenched Cu ZBA experiments and their 2CK interpretation. We first review the evidence that the ZBAs are due to electron scattering from structural defects that are not static, but possess internal dynamics. In order to distinguish between several mechanisms proposed to explain the experiments, we then analyze the scaling properties of the conductance at low temperature and voltage and extract from the data a universal scaling function $\mathcal{G}(v)$. The theoretical calculation of the corresponding scaling function within the 2CK model is the subject of papers II and III. The main conclusion of our work is that the properties of the quenched Cu data, and most notably their scaling behavior, are in good agreement with the 2CK model, and clearly different from several other proposed mechanisms.

Typeset using REVTeX

I. INTRODUCTION

The study of systems of strongly correlated electrons that display non-Fermi-liquid behavior has attracted widespread interest in recent years, fueled in part by their possible relevance to heavy-fermion compounds^{3–5} and high- T_c superconductivity materials^{6–8}. On the theoretical front, one of the consequences was a renewed interest in various multi-channel Kondo models, some of which were predicted by Nozières and Blandin⁹ to contain non-Fermi-liquid physics. Some of the most recent advances were made by Affleck and Ludwig (AL) (see¹⁰ and references therein), who developed an exact conformal field theory (CFT) solution for the $T = 0$ fixed point of the multichannel Kondo models. On the experimental front, an experiment performed by two of us (RB)^{1,11}, that investigated certain zero-bias anomalies (ZBAs) in the conductance of quenched Copper nanoconstrictions, has emerged as a potential experimental realization of the 2-channel Kondo (2CK) model and the corresponding non-Fermi-liquid physics^{2,12–14}. Although this interpretation has been greeted with scepticism by some^{15,16} and alternative mechanisms for the ZBAs have been proposed^{17,18}, the 2CK scenario has recently received important additional support from experimental results on ZBAs in metal break junctions^{19,20}.

In a series of three papers (I, II, III) we present a detailed analysis of these ZBA experiments and their 2CK interpretation. The present paper (I) is a comprehensive review of the quenched Cu ZBA experiments that attempts to integrate the results into a coherent picture (while postponing all formal theoretical developments to II and III). Paper II contains a calculation of the non-equilibrium conductance through a nanoconstriction containing 2CK impurities, which is compared with the Cu experiments. Paper III, which is the only paper of the three that requires knowledge of AL's conformal field theory solution of the 2CK model, describes a bosonic reformulation²¹ of their theory that is considerably simpler than those used previously and is needed to derive certain key technical results used in paper II.

Let us begin by briefly summarizing the quenched Cu ZBA experiments and how they inspired the theoretical work presented in papers II and III.

RB used lithographic techniques to manufacture quenched Cu constrictions of diameters as small as 3 nm (see Fig. 1), and studied the conductance $G(V, T, H)$ through the so-called nanoconstriction (or point contact) as a function of voltage (V), temperature (T) and magnetic field (H). Their constrictions were so small that they were able to detect electron scattering at the level of individual impurities or defects in the constriction. Since the energy dependence of the scattering rate can be extracted from the voltage dependence of the conductance, such an experiment probes the actual electron-impurity scattering mechanism.

For very small eV/k_B and T ($< 5K$), RB observed non-ohmic ZBAs in the voltage (V) and temperature (T) dependence of the conductance signals of unannealed, ballistic nanoconstrictions. The qualitative features of these anomalies (such as their behavior in a magnetic field, under annealing and upon the addition of static impurities), which are reviewed in detail in the present paper, lead to the proposal¹ that the ZBAs are caused by a special type of defect in the nanoconstrictions, namely two-level systems (TLSs). This proposal has recently received support from a related experiment by Keijsers *et al.* on nanoconstrictions made from metallic glasses^{19,20} (briefly reviewed in section VIII).

There are at least two theories for how TLSs can cause ZBAs in nanoconstrictions. In the first, based on Zawadowski's *non-magnetic Kondo model*^{22,23}, the interaction between

TLSs and conduction electrons is described, at sufficiently low energies, by the 2CK model (reviewed in Appendix B of paper II), leading to an energy dependent scattering rate and hence a ZBA. In the second, Kozub and Kulik's theory of *TLS-population spectroscopy*^{17,18}, the ZBA is attributed to a V -induced non-equilibrium occupation of the upper and lower energy states of the TLSs (see section V C).

Though the two theories make quite similar predictions for the shape of the ZBA, they make different predictions for the V/T -scaling behavior of $G(V, T)$. Whereas Kozub and Kulik's theory predicts that $G(V, T)$ does not obey any V/T -scaling relation at all, the 2CK scenario predicts² that in the regime $T \ll T_K$ and $eV \ll k_B T_K$ (where T_K is the Kondo temperature), the conductance $G(V, T)$ should obey a scaling relation of the following form:

$$\frac{G(V, T) - G(0, T)}{T^\alpha} = F(eV/k_B T) \quad (1)$$

where $F(x)$ is a sample-dependent scaling function. Moreover, AL's CFT solution of the 2CK problem suggested that by scaling out non-universal constants, it should be possible to extract a *universal*, (i.e. sample-independent) scaling curve, $\mathcal{G}(x)$ from $F(x)$, and that the conductance exponent α should have the universal non-Fermi-liquid value $\alpha = \frac{1}{2}$, in striking contrast to the usual Fermi-liquid value²⁴ of $\alpha = 2$. Since no calculation had been provided in Ref.² to support the statement that $\alpha = \frac{1}{2}$, its status up to now has been that of an informed guess rather than a definite prediction, a situation that is remedied in papers II and III.

A detailed scaling analysis² showed that the data of RB indeed do obey the above scaling relation, with $\alpha = 0.5 \pm 0.05$. It should be emphasized that the verification of scaling is a very significant experimental result: firstly, the scaling relation (1), by combining the V - and T -dependence of $G(V, T)$ for arbitrary ratios of V/T , contains much more information than statements about the separate V - or T -dependence would; and secondly, an accurate experimental determination of the scaling exponent α is possibly only by a scaling analysis of all the data (for a detailed review of this central ingredient of the data analysis, see section VII). Accurate knowledge of α is very important, since α succinctly characterizes the low-energy critical properties of the physics, enabling one to eliminate many otherwise plausible candidate theories for the ZBA (such as that by Kozub and Kulik).

The experimental value for α agrees remarkably well with the CFT prediction of $\alpha = \frac{1}{2}$; furthermore, the scaling curve, $\mathcal{G}(x)$ was indeed the same for all three samples studied in detail, in accord with the CFT expectation that it should be universal and hence sample-independent. Thus, this result considerably strengthens the case for the 2CK interpretation of the RB experiment, within which the experimental demonstration that $\alpha = \frac{1}{2}$ is, remarkably, equivalent to the direct observation of non-Fermi-liquid physics.

Nevertheless, this scaling behavior can conceivably also be accounted for by some other theory. Indeed, Wingreen, Altshuler and Meir^{15,(a)} have pointed out that an exponent of $\alpha = \frac{1}{2}$ also arises within an alternative interpretation of the experiment, based not on 2CK physics but the physics of disorder. (We believe that this interpretation is in conflict with other important experimental facts, see section V A).

It is therefore desirable to develop additional quantitative criteria for comparing experiment to the various theories. One possible criterion is the scaling function, $\mathcal{G}(x)$. A very stringent quantitative test of any theory for the RB experiment would therefore be to calculate the universal scaling function, $\mathcal{G}(x)$, which should be a fingerprint of the theory, and

compare it to experiment. Papers II and III are devoted to this task: $\rho(x)$ is calculated analytically within the framework of the 2CK model and its exact CFT solution by AL, and the results are compared to the RB experiment. When combined with recent numerical results of Hettler *et al.*¹², agreement with the experimental scaling curve is obtained, thus lending further quantitative support to the 2CK interpretation for the Cu constrictions.

The main conclusion of our work is that the 2CK interpretation can qualitatively and quantitatively account for all the scaling properties of the conductance measured in the ZBAs of Cu point contacts. The experiments by Keijsers *et al.*²⁰ on metallic-glass nanoconstrictions add further evidence in support of the 2CK interpretation, as opposed to other proposed mechanisms. However, we shall note that the 2CK model does not account for two phenomena observed in the quenched Cu samples. Firstly, the magnetic field dependence of the low-bias conductance is rather strong (the 2CK explanation for the field dependence that was offered in Ref.² does not seem to survive closer scrutiny, as discussed in section IX). Secondly, the conductance undergoes very sudden transitions at certain voltages V_c ^{11,25} (see (P9) of section IV), if T and H are sufficiently small. These voltages can be rather large (V_c typically ranges between 5 and 20 mV), implying that some new, large energy scale is involved. These two phenomena are not generic to TLS-induced ZBAs, however, since they are not observed in metallic-glass constrictions. We shall suggest that the two phenomena involve “high-energy” physics associated with the strongly-interacting system of electrons and atomic tunneling centers. Such physics is beyond the scope of the existing 2CK model and its CFT treatment, which deals only with the “low-energy” aspects of the problem.

Paper I is organized as follows: In section II we describe the fabrication and characterization of nanoconstrictions, and summarize some elements of ballistic point contact spectroscopy in section III. In section IV we summarize the main experimental facts associated with the ZBA in the Cu samples, which we state in the form of nine properties, (P1) to (P9). Section V describes arguments for ruling out a number of possible explanations for the ZBA that come to mind. The 2CK interpretation is presented in section VI, where its assumptions are summarized and critically discussed. Section VII contains a scaling analysis of the $G(V, T)$ data at $H = 0$. A related ZBA experiment on metallic-glass nanoconstrictions is briefly discussed in section VIII. Possible sources of magnetic field dependence in the 2CK scenario are discussed in section IX. Finally, we summarize the results and conclusions of this paper in section X.

II. THE NANOCONSTRICTION

A schematic cross-sectional view of a typical nanoconstriction (often also called a *point contact*) is shown in Fig. 1. The device is made in a sandwich structure. The middle layer is an insulating Si_3N_4 membrane. This contains in one spot a bowl-shaped hole, which just breaks through the lower edge of the membrane to form a very narrow opening, as small as 3 nm in diameter. The narrow neck at the lower opening in the Si_3N_4 membrane is so small that this region completely dominates the resistance, measured between the top and bottom of the structure. Only metal within a distance equal to a few constriction diameters from the narrowest region contributes significantly to the resistance signal. The small physical size of the structure serves to focus electrons so that only atoms in a very small region contribute to the resistance, and the resistance is sensitive to scattering from single defects

in the constriction region.

To fabricate the devices, electron beam lithography and reactive ion etching are used to form the bowl-shaped hole in a Si_3N_4 membrane. The technique for making a bowl-shaped hole that just breaks through the Si_3N_4 membrane (which is essential to obtaining a nano-hole) was developed by Ralls²⁶; the details relevant to the present experiments are described in Ref.^{11,section2.2}. In ultra-high vacuum ($< 2 \times 10^{-10}$ torr) and at room temperature the membrane is then rotated to expose both sides while evaporating metal to fill the hole (thus forming a metallic channel through the constriction) and coat both sides of the membrane. A layer of at least 2000 Å of metal is deposited on both sides of the membrane to form clean, continuous films. The phenomena discussed in this paper have been observed in Cu, Al, Ag, and Pt devices. They are observed only in devices which have been “quenched” – cooled to cryogenic temperatures shortly after being made by evaporation. The ZBA signals disappear in devices that are allowed to anneal. The time scale required for this annealing process varies from material to material, from several hours in Cu to several weeks for refractory metals.

III. BALLISTIC POINT CONTACT SPECTROSCOPY

A constriction is called *ballistic* if electrons travel ballistically through it, along semi-classical, straight-line paths between collisions with defects or the walls of the constriction. This occurs if two conditions are fulfilled: Firstly, it must be possible to neglect effects due to the diffraction of electron waves, i.e. one needs $1/k_F \ll a$, where a = constriction radius. Secondly, the constriction must be rather clean (as opposed to disordered): an electron should just scatter off impurities once or twice while traversing the hole. One therefore needs $a \ll l$, where l is the electron mean free path.

The quenched Cu ZBA-devices of RB reasonably meet both conditions: firstly, for Cu $1/k_F \simeq 0.1\text{nm}$, whereas a is of order 2-8 nm [as determined from the Sharvin formula for the conductance, Eq. (3)]. Secondly, for clean, annealed devices $l \sim 200$ nm (as determined from the residual bulk resistivity). For devices containing structural defects, l is reduced to about $l \gtrsim 30$ nm [see (P4)], which is still about twice the constriction diameter. Thus, we shall henceforth regard the quenched Cu ZBA-devices as ballistic constrictions.

Some aspects of the theory of transport through ballistic constrictions^{27,28} are reviewed in Appendix A of paper II. Here we merely summarize the main conclusions.

The differential conductance has the general form

$$G(V) \equiv \left| \frac{dI(V)}{dV} \right| = G_o + \Delta G(V). \quad (2)$$

The constant G_o , the so-called Sharvin conductance, arises from electrons that travel ballistically through the hole without scattering. Sharvin showed that for a round hole,

$$G_o = a^2 e^2 m \varepsilon_F / (2\pi \hbar^3), \quad (3)$$

where a is the radius of the hole, and hence the measured value of G_o can be used to estimate the size of the constriction.

Any source of scattering in the constriction that backscatters electrons and hence prevents them from ballistically traversing the hole gives rise to a backscattering correction ΔG . If the electron scattering rate $\tau^{-1}(\varepsilon)$ is energy-dependent, $\Delta G(V)$ is voltage dependent. In fact, one of the most important characteristics of ballistic nanoconstrictions is that the energy dependence of $\tau^{-1}(\varepsilon)$ can be directly extracted from the voltage dependence of $\Delta G(V)$, which implies that ballistic nanoconstrictions can be used to do spectroscopy of electron-defect scattering.

If, for example, the voltage is large enough to excite phonons ($> 5\text{mV}$ for Cu), the I - V curve is dominated by electron-phonon scattering. In this case, it can be shown that at $T = 0$, $\Delta G = -\left(\frac{4e^2 m^2 v_F a^3}{3\pi\hbar^4}\right) \tau^{-1}(eV)$ where $\tau^{-1}(\varepsilon') \equiv \int_0^{\varepsilon'} d\varepsilon \alpha^2 F_p(\varepsilon)$ is the relaxation rate for an electron at energy ε' above the Fermi surface. Thus, due to phonon-backscattering processes, the conductance of any point contact drops markedly at voltages large enough to excite phonons [$V > 5\text{ meV}$ for Cu, see Fig. 2(a)]. Furthermore, the function $\alpha^2 F_p(eV)$, the so-called *point contact phonon spectrum*, can be directly obtained from $\partial_V \Delta G(V)$. For any clean, ballistic Cu nanoconstriction, it should give the same function, characteristic of the phonon spectrum, and indeed nanoconstriction measurements thereof agree with other determinations of $\alpha^2 F_p$. However, the amplitude of the phonon-induced peaks is reduced dramatically if there is significant elastic scattering due to defects or impurities in the constriction region, as has been modeled theoretically²⁹ and demonstrated experimentally³⁰. Therefore, comparing the point contact phonon spectrum of a given point contact to the reference spectrum of a clean point contact provides an important and reliable tool for determining whether the point contact is clean or not.

For voltages below the phonon threshold ($V < 5\text{mV}$ for Cu), the V -dependence of $\Delta G(V)$ is due to scattering off defects. For a set of defects at positions \vec{R}_i , with an isotropic, elastic, but energy-dependent scattering rate $\tau^{-1}(\varepsilon)$, the backscattering conductance has the following form¹⁴:

$$\Delta G(V) = -(\tau(0)e^2/h) \int_{-\infty}^{\infty} d\omega [-\partial_\omega f_o(\hbar\omega)] \sum_i b_i \frac{1}{2} \left[\tau^{-1}(\hbar\omega - \frac{1}{2}eVa_i^+) + \tau^{-1}(\hbar\omega - \frac{1}{2}eVa_i^-) \right]. \quad (4)$$

We factorized out the constant $\tau(0)e^2/h$ to ensure that ΔG has the correct dimensions and order of magnitude. We assume that the resistance contribution from each defect may be calculated independently – that is, we ignore quantum interference for electrons scattering from multiple defects. The a_i and b_i are (unknown) constants of order unity that characterize all those details of scattering by the i -th impurity that are energy-independent and of a sample-specific, geometrical nature. The b_i account for the fact that the probability that an electron will or will not traverse the hole after being scattered off the i -th impurity depends on the position of the impurity relative to the hole. The a_i account for the fact that impurities that are at different positions \vec{R}_i in the nanoconstriction feel different effective voltages (because the amount by which the non-equilibrium electron distribution function at \vec{R}_i differs from the equilibrium Fermi function f_o depends on \vec{R}_i).

In spite of the presence of the many unknown constants a_i , b_i , we shall see that it is nevertheless possible to extract general properties of $\tau^{-1}(\varepsilon)$ from the measured $\Delta G(V, T)$ data. For example, from Eq. (4) one can deduce that if

$$\tau^{-1}(\varepsilon, T) - \tau^{-1}(0, T) \propto \begin{cases} \ln[\max(T, \varepsilon)], \\ T^\alpha \tilde{}(\varepsilon/T), \end{cases} \quad \text{then} \quad \Delta G(V, T) \propto \begin{cases} \ln[\max(T, V)], \\ T^\alpha F(V/T), \end{cases} \quad (5)$$

where $\tilde{}$ and F are scaling functions.

IV. EXPERIMENTAL FACTS FOR QUENCHED CU SAMPLES

In this section we summarize in brief the experimental facts relevant to the ZBA in quenched Cu samples. Our interpretation of these facts is postponed to later sections, where some of them will be elaborated upon more fully, and where most of the figures quoted below can be found.

The phenomenon to be studied is illustrated by the upper differential conductance curve in Fig. 2. Its three essential features are the following: Firstly, the differential conductance shows a drop for $|V| > 5$ mV, due to the excitation of phonons, a process which is well understood (see section III). Secondly, there are sharp voltage-symmetric conductance spikes at somewhat larger voltages (V_c), called *conductance transitions* in Ref.^{1,31}, because in the DC conductance they show up as downward steps with increasing V (see figure 13 below). Some of their complex properties are listed in point (P9) below.

Thirdly, the conductance has a voltage-symmetric dip in the conductance near $V = 0$; this is the so-called *zero-bias anomaly* (ZBA). As a sample is cooled, the temperature at which the zero-bias features become measurable varies from sample to sample, ranging from 10 K to 100 mK. This paper is concerned mainly with the regime $V < 5$ mV and this ZBA.

The ZBA is a very robust phenomenon. For decades it has been observed, but not carefully investigated, in mechanical “spear and anvil” point contacts made from a variety of materials, see e.g.³². Even the dramatic conductance transitions have probably been seen in early ZBA experiments²⁷, though their presence had not been emphasized there¹.

The advent of the mechanically very stable nanoconstrictions employed by RB allowed a detailed systematic study of the ZBA. Their findings are discussed at length in¹¹ and³¹. We summarize them in the form of 9 important properties of the ZBA in quenched Cu nanoconstrictions:

- (P1) *Quenching*: ZBAs and conductance transitions [Fig. 2(a)] are found only in *quenched* Cu samples, i.e. samples that are cooled to cryogenic temperatures within hours after being formed by evaporation. They are found in about 50% of such samples, and in a variety of materials, such as Cu, Al, Ag and Pt (Cu was used in the samples discussed below).
- (P2) *Amplitude*: Typical values for $G(V = 0)$ vary from 2000 to 4000 e^2/h . The anomaly is only a small feature on a very big background conductance: its amplitude [$G_{max} -$

¹For example, Fig. 3C of²⁷ shows a d^2I/dV^2 spectrum with sharp signals, more or less symmetric about zero, that are consistent with being derivatives of spikes in the dI/dV conductance curve. Note that these signals are too sharp to be spectroscopic signals smeared by kT , but are indicative of abrupt transitions.

$G(V=0)$] varies from sample to sample, from a fraction of e^2/h to as large as $70e^2/h$ at 100 mK. Its sign is always the same, with $G(V, T)$ increasing from $G(0, T_o)$ as V or T are increased. The sample (# 1 in Fig. 7) showing best scaling (see (P6) below) had a maximum ZBA amplitude of about $30e^2/h$.

(P3) *Annealing:*

(a) After annealing at room temperature for several days, the ZBA and conductance spikes disappear, and the conductance curve looks like that of a completely clean point contact [see lower curve in Fig. 2(a)].

(b) Nevertheless, such annealing changes the total conductance by not more than 1% or 2% (both increases and decreases have been observed), indicating that the overall structure of the constriction does not undergo drastic changes.

(c) Upon thermal cycling, i.e. brief (several minutes) excursions to room temperature and back, the amplitude of the ZBA and the V -position of the conductance transitions change dramatically and non-monotonically. [see Fig. 3(a)]. The complexity of this behavior suggests that the thermal cycling is causing changes in the position of defects within the constriction, and the ZBA is very sensitive to the precise configuration of the defects.

(P4) *Effect of disorder:*

(a) If static disorder is intentionally introduced into a nanoconstriction by adding 1% or more of impurity atoms such as Au to the Cu during evaporation, the zero-bias conductance dip and conductance spikes *disappear completely* [see Fig. 3(b)]. Likewise, the signals are absent in samples for which water is adsorbed onto the Si_3N_4 surface before metal deposition (the standard sample fabrication procedure therefore involves heating the sample to $\sim 100^\circ\text{C}$ in vacuum, or exposing it for several hours to ultraviolet light in vacuum, before the final metal evaporation is done).

(b) When a strongly disordered region is created near the constriction (by electromigration: a high bias (100-500 mV) is applied at low temperatures so that Cu atoms are moved around, a method controllably demonstrated in^{26,33,34}), the conductance shows no ZBA either, but instead small-amplitude, voltage-dependent (but aperiodic) conductance fluctuations at low voltage [see Fig. 3(c), (d)]. That these are characteristic of strongly disordered constrictions and can be interpreted as universal conductance fluctuations due to quantum interference, was established in a separate investigations^{35, 11,chapter 4, 36}.

(P5) *Phonon spectrum:* For quenched samples, in the point contact phonon spectrum the longitudinal phonon peak near 28 mV is not well-defined, and the total amplitude of the spectrum is smaller by about 15% than after annealing. After annealing, the longitudinal phonon peak reappears and the spectrum corresponds to that of clean ballistic point contacts. Both these differences indicate (see p. 6) that the elastic mean free path l in the annealed samples is somewhat longer than in the quenched samples. From the phonon spectrum of the latter, l can be estimated (see section II) to be $l \gtrsim 30$ nm [for the sample shown in Fig. 2(a)], still more than about twice the constriction diameter for that device. Note also that the point contact phonon

spectrum for a quenched device [Fig. 2(b)] is qualitatively very different from that of a strongly disordered constriction [Fig. 3(d)]. These facts, viewed in conjunction with (P3b) and (P4c), implies that the Cu constrictions displaying ZBAs are still rather clean and ballistic.

(P6) *V/T scaling* (to be established in detail in section VII):

(a) At $H = 0$, the conductance obeys the following scaling relation if both $V < V_K$ and $T < T_K$, but for arbitrary ratio $v = eV/k_B T$:

$$\frac{G(V, T) - G(0, T)}{T^\alpha} = F(v). \quad (6)$$

Relation (6) allows a large number of data curves to be collapsed onto a single, sample-dependent scaling curve [e.g. see Figs. 8(a) and 8(b) below]. The departure of individual curves from the low- T scaling curve in Figs. 8(a) and 8(b) indicates that V or T has surpassed the crossover scales V_K or T_K . From the data, these are related roughly by $eV_K = 2k_B T_K$, with T_K in the range 3 to 5 K.

(b) $F(v)$ is a sample-dependent scaling function with the properties $F(0) \neq 0$ and $F(v) \propto v^\alpha$ as $v \rightarrow \infty$, and the scaling exponent is found to have the value $\alpha = 0.5 \pm 0.05$.

(c) By scaling out sample-dependent constants, it is possible to extract from $F(v)$ a “universal” scaling function, $\tilde{F}(v)$ [shown in Fig. 11(b) below]. $\tilde{F}(v)$ is universal in the sense that it is indistinguishable for all three devices for which a scaling analysis was carried out (they are called sample 1,2 and 3 below).

(P7) *Logarithms*: For V or T beyond the cross-over scales V_K or T_K , $G(V, T)$ deviates markedly from the scaling behavior of (P6) and behaves roughly logarithmically: For $H = 0$ and fixed, small T , the conductance goes like $\ln V$ for $V > V_K$ [Fig. 5(a)]; similarly, for $H = V = 0$ and $T > T_K$, the conductance goes like $\ln T$ [Fig. 5(b)].

(P8) *Magnetic field*:

(a) When a magnetic field (of up to 6 T) is applied, the amplitude of the ZBA in Cu devices decreases [see Fig. 4(b)]. The change in amplitude can be as large as $24 e^2/h$ if H changes from 0 to 6 T. For sufficiently small H (< 1 T), at fixed T and $V = 0$, the magnetoconductance roughly follows $G(H, T) \propto |H|$ (see Fig. 14 below). However, the available data is insufficient to establish linear behavior beyond doubt, and, for example, would also be compatible with a $|H|^{1/2}$ -dependence.

(b) The ZBA dip undergoes no Zeeman-splitting in H , in contrast to the Zeeman splitting that is found for devices intentionally doped with magnetic impurities such as Mn [see Fig. 4(a)].

(P9) *Conductance Transitions*:

(a) Voltage-symmetric conductance transitions (spikes in the differential conductance at certain “transition voltages” V_c , see Fig. 2) occur only in quenched point contacts that show ZBAs, but occur in at least 80% of these. The spikes disappear under annealing, just as the ZBA does (P3a).

(b) (i) A single sample can show several such conductance transitions (up to 6 different

V_c s have been observed in a single sample). (ii) If T and H are small (say $T \lesssim 1\text{K}$, $H \lesssim 0.5\text{T}$), V_c is typically rather large, with typical values ranging between 5 and 20 mV, well above the typical voltages associated with the ZBA (i.e. $V_c > V_K$). The spikes have a very complex behavior as a function of temperature (T) and magnetic field (H), including (iii) a hysteretic V -dependence, (iv) a bifurcation of single spikes into two separate ones (V_{c1}, V_{c2}) when $B \neq 0$ (Fig. 12), (v) the H -dependent motion of the spike positions $V_c(H) \rightarrow 0$ when H becomes sufficiently large (Figs. 12, 13), and (vi) a very rapid narrowing of the peaks with decreasing T . They are described at length, from a phenomenological point of view, in Ref.³¹.

Any theory that purports to explain the ZBA in Cu constrictions must be consistent with all of the above experimental facts. An extension of this list to include the results of the recent related ZBA experiment by Keijsers *et al.* on metallic-glass constrictions is presented in section VIII.

V. IN SEARCH OF A PLAUSIBLE INTERPRETATION

We shall argue that the most plausible interpretation of the above experimental facts is the 2CK interpretation, which attributes the ZBA to the presence of dynamic TLSs in the constriction. Before presenting this scenario in section VI, however, in the present section we first eliminate some other conceivable explanations.

A. Static Disorder

Could the ZBA be due to static disorder? For example, one could consider attributing the decreased conductance near $V = 0$ to either weak localization due to disorder³⁷ or disorder-enhanced electron-electron interactions³⁸. In fact, the latter possibility (first mentioned, but deemed implausible, in Ref.¹²), was recently advocated¹⁵ by Wingreen, Altshuler and Meir (WAM) (Ref.¹⁵ also contains a critique of a crucial assumption of the 2CK scenario, which is discussed in section VIC 3).

WAM made the interesting observation that if just the region of the device near to the point-contact orifice were highly disordered, this would give rise to a local depression in the density of states near the Fermi surface of the form $\delta N(\varepsilon - \varepsilon_F, T) \propto -T^{1/2} F\left(\frac{\varepsilon - \varepsilon_F}{T}\right)$, where F is a scaling function. This in turn would reduce the rate at which electrons incident ballistically into the disordered region could traverse the sample. The total conductance would hence be reduced by an amount $\Delta G(V, T) \propto \partial_V \int_{\varepsilon_F}^{\varepsilon_F + eV} d\varepsilon \delta N(\varepsilon - \varepsilon_F, T) = \delta N(V, T)$. Due to the scaling form of δN , this argument explains the scaling property (P6), and in fact the scaling curve $F(v)$ of Eq. (6) that it produces is in quantitative agreement with that of sample 1 (see^{15, Fig.1}). According to their estimates, this scenario would require a disordered region of diameter 50 nm (the size of the bowl), a mean free path $l = 3$ nm and a diffusion constant $D = 15 \text{ cm}^2/\text{s}$, i.e. rather strong disorder.

The WAM scenario is appealing in that it accounts for the unusual $T^{1/2}$ behavior using well-tested physical ideas, without having to evoke any exotic new physics (such as the non-Fermi liquid physics implied by the 2CK model advocated below). However, it is at odds with a number of qualitative (and hence very robust) properties of the ZBA^{11, section 6.6.1, 15,(b)}:

1. According to (P4a), upon the intentional introduction of static disorder the ZBAs are not enhanced, as one would have expected in WAM's static disorder scenario, but *disappear completely*, in contradiction to the latter.
2. The quenched Cu constrictions actually are considerably *cleaner* than is assumed in WAM's scenario, as can be seen from three separate arguments:
 - (a) According to (P5), a direct estimate of the mean free path, based on the point contact phonon spectrum (a reliable and well-tested diagnostic method^{27,28}) suggests $l \gtrsim 30$ nm instead of WAM's 3 nm.
 - (b) WAM attempted to explain (P3a), the disappearance of the zero-bias anomalies under annealing, by assuming that the presumed static disorder anneals away at room temperature. However, this suggestion fails a simple quantitative consistency check: let us model the constriction region by a Cu cylinder 40 nm in diameter and 40 nm long, with $l = 3$ nm. Estimating the resistance of this cylinder using the Drude model yields $R = 7\Omega$, which would be the dominant part of the resistance of the device ($R < 10\Omega$ in the lower- R devices). If annealing now removes sufficient disorder that the ZBA disappears, l would have to increase considerably, implying that the overall R of the device would necessarily decrease by tens of percent, which contradicts (P3b) (according to which resistance sometimes even increases under annealing).
 - (c) According to (P4b) even a somewhat smaller amount of disorder ($l = 7$ nm) than assumed by WAM has been observed to cause voltage dependent conductance fluctuations due to quantum interference. However, these tell-tale signs of static disorder were never seen in the quenched ZBA samples (P4c), though they did appear as soon as disorder was purposefully induced using electromigration (P4b). In other words, in Cu nanoconstrictions the signature of static disorder is conductance fluctuations, not a ZBA.
3. In the static disorder scenario, in which the conductance depends only on the *average* disorder in the bowl (not on the precise configuration of individual defects) it is unclear how to account for the complex behavior of the ZBA under thermal cycling (P3c).
4. The static disorder scenario provides no hint at all about the possible origin of the conductance transitions. WAM have suggested that these may be due to superconducting regions in the constriction (caused by an attractive electron-electron interaction at short range), but this suggestion fails to account for the presence of several different transitions in the same sample (moreover, superconductivity in a Cu sample seems highly implausible).
5. As first observed in¹², WAM's static disorder scenario provides no natural explanation for the $\ln V$ and $\ln T$ dependence of the conductance observed at energy scales above T_K (P7) (in contrast to the 2CK model discussed below). However, this objection is less compelling than the other ones above, because deviations from the scaling form of δN are expected at large energies, and the apparently logarithmic regime in the data is sufficiently small as to not be logarithmic beyond all doubt.

B. Magnetic Impurities

The asymptotic dependence of the conductance on $\ln V$ or $\ln T$ (P7) is reminiscent of the magnetic Kondo effect, where the resistance increases as $\ln T$ with decreasing T (as long as $T > T_K$). However, there are at least three strong arguments that rule out magnetic impurities as the source of the anomalies:

1. An effect due to magnetic impurities would not anneal away at higher temperatures (P3a), since magnetic impurities are stable within constrictions, not annealing away at room temperatures over a time scale of 6 months³¹.
2. If the magnetic Kondo effect were at work, a magnetic field would cause a well-known Zeeman splitting in the zero-bias conductance dip, as has been observed in nanoconstrictions intentionally doped with the magnetic impurity Mn^{11,section5.2}, as shown in Fig. 4(a). However, in the devices under present consideration, a Zeeman splitting has never been observed (P8b).
3. Magnetic impurities in metal break junctions have been observed to cause ZBAs that do not exhibit splitting because the Kondo temperature scale is larger than the Zeeman energy³⁹. However the ZBA signals caused by these impurities are very different than the ones we investigate, because they exhibit Fermi liquid scaling ($\alpha = 2$) rather than the $\alpha = 0.5$ we measure.

C. TLS population spectroscopy

Many of the qualitative features of the quenched Cu ZBAs can be understood within the framework of Kozub and Kulik's (KK) theory of TLS-population spectroscopy^{17,19}, which has recently been extended by Kozub, Rudin, and Schober¹⁸. This theory assumes that the constriction contains TLSs with non-zero energy splittings Δ_i , so that the application of a voltage will induce a non-equilibrium population $n_{i\pm}(V)$ of the higher and lower states $|\pm\rangle_i$ of each TLS (labelled by i). Assuming that these two states have different cross-sections σ_i^\pm for scattering electrons, the resistance $R(V)$ will then depend non-linearly on the voltage and temperature. According to Kozub and Kulik, the differential resistance has the form

$$\frac{1}{R} \frac{dR}{dV} = \sum_j \frac{eC_j}{2\Delta E_j} (\sigma_j^+ - \sigma_j^-) \tanh(\frac{1}{2}\tau^{-1}) S(\nu_j, \tau_j, q_j), \quad (7)$$

where $\nu_j = eV/\Delta E_j$, $\tau_j = k_B T/\Delta E_j$, E_j is the energy splitting and C_j and q_j are geometrical coefficients depending on the location of the i -th TLS in the constriction. The function $S(\nu, \tau, q)$, which they calculated explicitly, determines the shape of the differential resistance curve (see Fig. 2 of¹⁷), which can vary quite significantly, depending on the parameters q and τ . Note also that since the signs of $(\sigma_j^+ - \sigma_j^-)$ are arbitrary (except under special assumptions, see⁴⁰), Eq. (7) predicts that ZBAs of both signs should occur.

The shape of the ZBAs measured by RB are qualitatively of the same form as that predicted by KK's theory (which has significant freedom for curve-fitting, due to the undetermined parameters q_j and E_j). However, since the function depends on the two parameters

ν and τ separately, this theory cannot account for the existence of a scaling law found in (P6a), and certainly not for the specific value $\alpha = \frac{1}{2}$ of the scaling exponent (P6b).

Note, however, that Kozub and Kulik's theory cannot be ruled out as being part of the explanation of some some related ZBA experiments on nanoconstrictions made from disordered materials, such as those summarized in section VIII, since for these no scaling behavior has been reported to date.

D. Properties of external circuit

It was pointed out to us by G. Schön⁴¹ that fluctuations in the voltage V due to fluctuations in the external circuit can be shown to lead to a conductance $G(V, T)$ that satisfies the V/T -scaling behavior in (P6) (but with the exponent α determined by the external resistance of the circuit, and hence non-universal).

However, since the ZBAs only occur in quenched samples (P1), and since ZBAs anneal away at room temperature (P3a), they must be due to some internal properties of the sample. Hence they cannot be due to properties of the external electrical circuit, such as external voltage fluctuations.

E. Charge Traps and other Possibilities

The insulating material used in the devices, namely amorphous Si_3Ni_4 , may contain charge traps⁴², which could act as Anderson impurities or quantum dots through which conduction electrons could hop. This could cause dips in the differential conductance through several mechanisms, such as Kondo scattering from Anderson impurities⁴³, inelastic hopping conduction^{44,45} or Coulomb blockade effects⁴⁶.

However, charge traps can be ruled out for the present experiments for the following reason. A charge trap has in fact been unambiguously observed in a different experiment by Ralph and Buhrman²⁵. The conductance shows a very characteristic *peak* at $V = 0$, in complete contrast to the ZBA-dip. The suggestion of Ref.²⁵ that this is a Kondo peak that can be associated with Anderson hopping of electrons through the trap was taken up by König *et al.*⁴⁷, who calculated the conductance $G(V, T)$ for this scenario and found reasonably good agreement with that experiment. In other words, if charge traps are present, their signals are unmistakable, and very different from the ZBAs of present interest.

Other reasons ruling out charge traps as causes for the ZBAs may be found in^{11,section6.6.2}. Also in^{11,section6.6} a number of other mechanisms were also considered and ruled out as causes for the observed ZBAs: electronic surface states or quasi-localized states within the metal, defect rearrangement, mechanical instabilities, superconducting phases and heating effects.

VI. THE 2-CHANNEL KONDO (2CK) INTERPRETATION

In this section, we develop the 2CK interpretation of the ZBAs in quenched Cu constrictions. *It attributes the ZBA to the presence in the constriction region of structural defects, namely TLSs, that interact with conduction electrons according to the non-magnetic Kondo model, which renormalizes at low energies to the non-Fermi-liquid regime of the 2CK*

model. We begin by briefly recalling in section VI A some properties of two-level systems (or slightly more generally, dynamical two-state systems) in metals. Successes and open questions of the 2CK scenario are discussed in subsections VI B and VI C, respectively, and its key assumptions are listed, in the form of a summary, in subsection VI D.

A. Two-state systems

A dynamical two-state system (TSS), is an atom or group of atoms that can move between two different positions inside a material⁴⁸. In the absence of interactions, its behavior is governed by a double well potential, generically depicted in Fig. 6, with asymmetry energy Δ_z , tunneling matrix element Δ_x . The corresponding Hamiltonian is

$$H_{TSS} = \frac{1}{2} (\Delta_z \tau^z + \Delta_x \tau^x) , \quad (8)$$

where τ^x and τ^z are Pauli matrices acting in the two-by-two Hilbert space spanned by the states $|L\rangle$ and $|R\rangle$, describing the fluctuator in the left or right well.

Depending on the parameters of the potential, the atom's motion between the potential wells is classified as either slow, fast or ultrafast, with hopping rates $\tau^{-1} < 10^8 s^{-1}$, $10^8 s^{-1} < \tau^{-1} < 10^{12} s^{-1}$ or $\tau^{-1} > 10^{12} s^{-1}$, respectively⁴⁹. *Slow* two-state systems, called *two-state fluctuators*, have large barriers and negligibly small Δ_x , and the motion between wells occurs due to thermally activated hopping or incoherent quantum tunneling. *Fast* two-state systems have sufficiently small barriers and sufficiently large Δ_x that *coherent tunneling* takes place back and forth between the wells. Such a system is known as a *two-level tunneling system* (TLS), because its physics is usually dominated by its lowest two eigenstates (even and odd linear combinations of the lowest-lying eigenstates of each separate well), whose eigenenergies differ by $\Delta = (\Delta_z^2 + \Delta_x^2)^{1/2}$. *Ultra-fast* two-state systems have such a large Δ_x that Δ too becomes very large, so that at low temperatures only the lowest level governs the physics.

1. Slow Fluctuators

The fact that two-state systems in metal nanoconstrictions can influence the conductance was demonstrated by Ralls and Buhrman^{33,34,36}, who observed so-called telegraph signals in *well-annealed* devices (at rather high temperatures of 20-150K). These are slow, time-resolved fluctuations (fluctuation rates of about $10^3 s^{-1}$) of the conductance between two (or sometimes several) discrete values, differing by fractions of e^2/h , which can be attributed to the fluctuations of a *slow* two-state fluctuator in the constriction region.

Such telegraph signals were also observed by Zimmerman *et al.*^{50,51}, who studied the conductance of polychrystalline Bi films, a highly disordered material with presumably large numbers of two-state systems. They were able to measure the parameters of individual slow fluctuators directly, finding values for the asymmetry energy Δ_z ranging from as little as 0.08 K to about 1K. They also demonstrated that in a disordered environment the asymmetry energy of a TLS is a random, non-monotonic function² of the magnetic field, $\Delta_z = \Delta_z(H)$

²The reason is, roughly, that Δ_z depends on the difference $\delta\rho$ in the local electron density at the

(as predicted earlier in Ref.⁵²), and hence can be “tuned” at will by changing H .

Unfortunately, experiments on *slow* fluctuators do not yield any direct information on the parameters to be expected for fast ones, since their parameters fall in different ranges.

2. Two-Level Systems

Fast fluctuators or TLSs presumably have the same microscopic nature and origin as slow fluctuators, being composed of atoms or small groups of atoms which move between two metastable configurations, but with much lower barriers. Therefore, they anneal away quicker than slow fluctuators, which is why they were not seen in the above-mentioned Ralls-Buhrman experiments on well-annealed samples^{11,p. 265}. Also, whereas slow fluctuators “freeze out” as T is lowered (which is why they don’t play a role in the ZBA regime of $T < 5\text{K}$), at low T fast fluctuators continue to undergo transitions by tunneling quantum-mechanically between the wells.

A fast fluctuator or TLS interacting with conduction electrons is usually described by the *non-magnetic* or *orbital Kondo model*, studied in great detail by Zawadowski and coworkers^{22,23} (it is defined and reviewed in more detail in Appendices B and C of paper II; for other reviews, see^{53,49}):

$$H = H_{TSS} + \sum_{\vec{k}} \varepsilon_{\vec{k}} c_{\vec{k}\sigma}^\dagger c_{\vec{k}'\sigma} + \sum_{\vec{k}\vec{k}'} c_{\vec{k}\sigma}^\dagger \left[V_{\vec{k}\vec{k}'}^0 + V_{\vec{k}\vec{k}'}^x \tau^x + V_{\vec{k}\vec{k}'}^z \tau^z \right] c_{\vec{k}'\sigma}. \quad (9)$$

Here $c_{\vec{k}\sigma}^\dagger$ creates an electron with momentum \vec{k} and Pauli spin σ . The terms V^0 and $V^z \tau^z$ describe *diagonal* scattering events in which the TLS-atoms do not tunnel between wells. The term $V^x \tau^x$ describes so-called *electron-assisted tunneling* processes. During these, electron scattering does lead to tunneling, and hence the associated bare matrix elements are much smaller than for diagonal scattering: $V^x/V^z \simeq 10^{-3}$.

Zawadowski and coworkers showed that the electron-assisted term $V^x \tau^x$ renormalizes to substantially larger values as the temperature is lowered (as does a similar $V^y \tau^y$ term that is generated under renormalization). At sufficiently low temperatures (where $V^z \simeq V^x \simeq V^y$), the non-magnetic Kondo model was shown⁵⁴ to be equivalent to the standard 2-channel Kondo (2CK) model, with an effective interaction of the following form:

$$H_{int}^{eff} = v_K \int d\varepsilon \int d\varepsilon' \sum_{\alpha,\alpha'} \sum_{\sigma\sigma'} c_{\varepsilon\alpha\sigma}^\dagger \left(\frac{1}{2} \vec{\sigma}_{\alpha\alpha'} \cdot \frac{1}{2} \vec{\tau} \right) c_{\varepsilon\alpha'\sigma}. \quad (10)$$

The two positions of the fast fluctuator in the L - and R wells correspond to the spin up and down of a magnetic impurity (and L - R transitions to impurity spin flips). The electrons are labelled by an energy index ε , a so-called pseudo-spin index $\alpha = 1, 2$ (corresponding to those two combination of angular momentum states about the impurity that couple most strongly to the TLS), and the Pauli spin index $\sigma = \uparrow, \downarrow$. Evidently, α plays the role of the

two minima of the TLS potential. Due to quantum interference effects that are amplified by the presence of disorder, changes in H can induce random changes in $\delta\rho$ and hence also in Δ_z .

electron's magnetic spin index in the magnetic 2CK model, and since the effective interaction is diagonal in σ (which has two values), σ is the channel index.

This (non-magnetic) 2CK model, with strong analogies to the magnetic one, yields an electron scattering rate $\tau^{-1}(\varepsilon, T)$ with the properties^{23,55}

$$\tau^{-1}(\varepsilon, T) - \tau^{-1}(0, T) \propto \begin{cases} \ln [\max (T, \varepsilon)] & \text{if } T > T_K, \\ T^{1/2}, \tilde{\sim} (\varepsilon/T) & \text{if } \Delta^2/T_K < T \ll T_K. \end{cases} \quad (11)$$

(The condition $\Delta^2/T_K < T$ is explained in section VII C.) Hence, for $T > T_K$ or $\Delta^2/T_K < T \ll T_K$, it yields [via Eq. (5)] a contribution to the conductance of $\delta\sigma(T) \propto \ln T$ or $T^{1/2}$, respectively. The latter is typical for the complicated non-Fermi-liquid physics characteristic of the 2CK model in the $T \ll T_K$ regime. In this respect the non-magnetic 2CK model differs in an important way from the (1-channel) magnetic Kondo model, for which the low- T scaling is of the Fermi liquid form ($\propto T^2$).

B. Successes of the 2CK Interpretation

We now turn to an interpretation of facts (P1) to (P9) in terms of the 2CK scenario^{1,2}. Our aim here is to sketch the physical picture underlying the scenario. Those aspects that require detailed analysis, such as the scaling behavior (P6) and magnetic field dependence (P8), will be discussed more fully in subsequent sections.

Qualitative features: The cooling and annealing properties (P1) and (P3) suggest that the ZBAs are due to *structural* defects or disorder that can anneal away at high temperatures [although the well-resolved phonon spectrum implies that only a small amount of such disorder can be present (P5)]. This conclusion is reinforced by the remarkably complex and non-monotonic behavior of the ZBA under thermal cycling (P3c), which indicates that the ZBA probes the detailed configuration of individual defects, not just the average behavior of the entire constriction region.

By assuming that the ZBA is due to fast TLSs, i.e. a specific type of structural defect, the 2CK scenario accounts for all of the properties just mentioned. Property (P4a), the disappearance of the ZBA upon the addition of 1% Au atoms, can then be attributed to the TLSs being pinned by the additional static impurities.

Logarithms and Scaling: Next, we assume that the TLS-electron interaction is governed by Zawadowski's non-magnetic Kondo model, which renormalizes to the 2CK model at low energy scales. This explains a number of further facts. Firstly, the non-magnetic nature of the interaction explains the absence of a Zeeman splitting in a magnetic field (P8b). Furthermore, the fact that the 2CK scattering rate $\tau^{-1}(\varepsilon, T)$ has a logarithmic form for $\varepsilon > T_K (> T)$ or $T > T_K (> \varepsilon)$ [see Eq. (11)] accounts, via Eq. (5), for the asymptotic logarithmic V - and T dependence (P7) of $G(V, T)$ for $V > V_K (> T)$ or $T > T_K (> V)$. Thus, we identify the experimental crossover temperature T_K ($\simeq 3$ to 5 K) of (P6a) with the Kondo temperature of the 2CK model.

Similarly, the scaling form of $\tau^{-1}(\varepsilon, T)$ for $\varepsilon, T \ll T_K$ [see Eq. (11)] accounts, via Eq. (5), for the observed scaling behavior (P6) of $G(V, T)$ for $V < V_K$ and $T < T_K$. To be more particular, the very occurrence of scaling behavior (P6a), and fact that the experimental scaling curve, (v) of (P6c) is universal, can be explained (see section VII A) by assuming

that the system is in the neighborhood of some fixed point. Assuming this to be the 2CK non-Fermi-liquid fixed point, the experimentally observed scaling regime can be associated with the theoretical expected scaling regime of $\Delta^2/T_K < T \ll T_K$ and $V \ll T_K$. Moreover, the non-Fermi-liquid value of $\alpha = \frac{1}{2}$ that is then expected for the scaling exponent (see section VII A) agrees precisely with the value observed for α . Thus, within the 2CK interpretation, the experimental demonstration of $\alpha = \frac{1}{2}$ is equivalent to the direct observation of non-Fermi-liquid behavior. Finally, it will be shown in paper II that the shape of the universal scaling curve, (v) is also in quantitative agreement with the 2CK model.

Number of TLSs: Each 2CK impurity in the constriction can change the conductance by at most $2e^2/h$.³ Therefore, the sample with the largest ZBA of $70e^2/h$ (sample # 2 in Fig. 7) would require up to about 40 such TLSs in the constriction. However, this is still only a relatively small amount of disorder (corresponding to a density of about 10^{-4} TLSs per atom^{11,p.2774}). The sample that showed the best scaling (sample # 1 in Fig. 7) had a significantly smaller amplitude of $\lesssim 20e^2/h$, implying only about 10 active TLSs.

C. Open Questions in the 2CK Scenario

Having discussed the successes of the 2CK scenario, we now turn to questions for which the 2CK scenario is unable to offer a detailed explanation, namely the conductance transitions (P9), the strong magnetic field dependence (P8a), and the microscopic nature of the TLSs. We shall point out below that (P9) and (P8a) are not generic to TLS-induced ZBAs, and speculate that they are related and must involve some new “high-energy” physics, since (P9) occurs at a large voltage V_c . Therefore, our lack of understanding of the latter need not affect the 2CK interpretation of the low-energy scaling behavior (P6). We conclude with some speculations about the microscopic nature of the TLSs, and the likelihood that realistic TLSs will have all the properties required by the 2CK scenario.

1. Conductance Transitions

The fact that conductance transitions occur only in samples that have a ZBA (P9a) suggests³¹ that these are related to the ZBA: if the latter is phenomenologically viewed as the

³To see this, we note that in the unitarity limit the scattering rate of electrons off a k -channel Kondo defect is proportional to $k \sin^2 \delta$ (see e.g.^{56,Eq.(2.20)}), and the phase shift at the intermediate-coupling fixed point is $\delta = \pi/2k$ ⁵⁷. Thus, in the unitarity limit, the contribution to the resistance of a $k = 2$ Kondo impurity is the same as for $k = 1$, namely $2e^2/h$ (the 2 comes from Pauli spin).

⁴For example, the 6.4Ω constriction studied in¹ has a diameter of ~ 13 nm [estimated via the Sharvin formula Eq. (3)], and there are 10^5 Cu atoms within a sphere of this diameter about the constriction. Assuming on the order of ~ 40 active TLSs, their density is therefore roughly of order 10^{-4} /atom. Although the constriction is believed to be crystalline, not glassy, it is worth noting that this density of TLSs is about the same as estimates for the total density of TLSs in glassy systems.

manifestation of some strongly correlated state of the system then conductance transitions corresponds to the sharp, sudden, “switching off” of the correlations as V becomes too large. For example, in the 2CK interpretation, interactions of electrons with TLSs in the constriction give rise to a strongly correlated non-Fermi-liquid state at small T and V . One might speculate that if for some reason a large voltage could “freeze” the TLSs, i.e. prevent them from tunneling, this would disrupt the correlations and give rise to a sudden change in the DC conductance and hence a spike in the differential conductance.

At present we are not aware of any detailed microscopic explanation for the conductance transitions. However, recent experiments by Keijsers, Shklyarevskii, and van Kempen¹⁹ on constrictions made from metallic glasses [reviewed in section VIII, see (P13)] showed TLS-induced ZBAs with properties very similar to RB’s quenched Cu constrictions, but no conductance transitions at all. This suggests that conductance transitions are *not* a generic ingredient of the phenomenology of ZBAs induced by TLSs. Moreover, in the quenched Cu samples, provided that H and T are sufficiently small, the transition voltage V_c at which the first conductance transition occurs usually lies well above T_K , the scale characterizing the extent of the low-energy scaling regime of the ZBA [see Fig. 2(a)]. (In other words, since they don’t occur near zero bias, the conductance transitions need not be viewed as part of the zero-bias anomaly phenomenon at all, if one restricts this term to refer only to the low-energy regime.)

Thus, there seems to be a clear separation of energy scales governing the ZBA and the conductance transitions. The latter must therefore be governed by some new large energy scale due to a mechanism not yet understood [but speculated about in section IX]. However, due to the separation of energy scales, the conductance transitions need not affect our description of the low-energy scaling regime of the ZBA below T_K (which is $\ll eV_c/k_B$) in terms of the 2CK model.

2. Strong Magnetic Field Dependence

Since the electron-TLS interaction is non-magnetic, i.e. not directly affected by a magnetic field, the 2CK scenario predicts no, or at best a very weak magnetic field dependence for the ZBA. This agrees with the absence of a Zeeman splitting of the ZBA for the Cu samples (P8b) (which was in fact one of the main reasons for the proposal of the non-magnetic 2CK interpretation¹). However, it leaves the strong magnetic field dependence (P8a) as a puzzle. In section IX we shall investigate two indirect mechanism for H to couple to a 2CK system, namely via H -tuning of the asymmetry energy $\Delta_z(H)$ and via channel symmetry breaking, but shall find that both are too weak to account for (P8a).

It is therefore very significant that the experiments by Keijsers *et al.* on metallic-glass nanoconstrictions show a ZBA which does not have any H -dependence [see section VIII, (P12)], in accord with 2CK expectations. This suggests that, just as the conductance transitions, the strong magnetic field dependence (P8a) of the quenched Cu constrictions are *not* a generic feature of TLS-induced ZBAs. Moreover, Fig. 13 suggests that in the Cu samples these two properties might be *linked*:, because it shows that the strong H -dependence of $G(V = 0, H)$ is related to the fact that the transition voltage V_c decreases to 0 as H is increased (P9b,v). (In other words, if the strongly correlated state sets in at

smaller V_c as V is lowered, the voltage-regime $0 < V < V_c$ in which the anomaly can develop is smaller, so that its total amplitude is smaller.)

Since the main difference between the Cu and the metallic-glass constrictions seems to be that the former contain TLSs with very small Δ 's, whereas in metallic glasses there will certainly be a broad distribution of splittings, we speculate that the conductance spikes and strong H -dependence might both be a consequence of the very small Δ s occurring in the Cu samples, perhaps due to interactions between several TLSs with very small splittings.

Thus, we conclude that attempts (such as those in²) to explain the H -dependence of the ZBA (even at $V = 0$) purely in terms of the 2CK model, which captures only the physics at low energies below T_K , are misdirected, because the H -dependence would arise, via the conductance transitions, from the “high-energy” physics associated with the large scale V_c .

This interpretation, according to which a magnetic field does not directly affect the low-energy physics of the phenomenon (only indirectly via its effect on V_c), can be checked by doing a V/T scaling analysis at fixed but small, non-zero magnetic field. If H is sufficiently small that the conductance transitions still occur at relatively high voltages (i.e. $V_c > T_K$), the scaling properties of (P6) should not be affected by having $H \neq 0$). Unfortunately, at present insufficient data is available to test this prediction.

The conclusions of this and the previous subsection are summarized in assumptions (A4) and (A5) in subsection VID.

3. Microscopic Nature of the TLS

Finally, the 2CK interpretation is of course unable to answer the question: What is the microscopic nature of the presumed TLSs? Now, ignorance of microscopic details does not affect our explanation for why the scaling properties (P6) of the ZBA seem to be universal: because the latter are presumably governed by the *fixed point* of the 2CK model, any system that is somewhere in the vicinity of this fixed point will flow towards it as the temperature is lowered (provided that relevant perturbations are sufficiently small) and hence exhibit the same universal behavior, irrespective of its detailed bare parameters.

However, the quality of the scaling behavior implies some rather stringent restrictions on the allowed properties of the presumed TLSs, because we need to assume that all active TLSs (e.g. about 10 for sample # 1, which shows the best scaling) are close enough in parameter space to the non-Fermi-liquid fixed point to show pure scaling.

This implies, firstly, that interactions between TLSs (which are known to exist in general³³, mediated by strain fields and changes in electron density), must be negligible, because they would drive the system away from the 2CK non-Fermi-liquid fixed point. Secondly, the fact that scaling is only expected in the regime $\Delta^2/T_K < T \ll T_K$ can be used to estimate that $T_K \simeq 3$ to 5K and $\Delta \lesssim 1$ K (see section VII for details). Kondo temperatures in the range of 1-10 K are in good agreement with the most recent theoretical estimates for TLSs⁵⁸. However, the condition $\Delta \lesssim 1$ K implies that for active TLSs the distribution of energy splittings, $P(\Delta)$, must be peaked below $\Delta \lesssim 1$ K. Since $\Delta = (\Delta_z^2 + \Delta_x)^{1/2}$, both the asymmetry energy Δ_z and tunneling rate Δ_x must be $\lesssim 1$ K, a value so small that it needs further comment.

First note that it is not immediately obvious that values of the bare tunneling rate Δ_x exist at all that allow 2CK physics: For transitions to be able to take place, the barrier

between the wells must be sufficiently small, but a small barrier is usually associated with a large bare Δ_x , implying a large bare Δ (and Δ sets the energy scale at which the renormalization flow toward the non-Fermi-liquid fixed point is cut off). Now, for a TLS in a metal, the physics of screening can reduce the direct tunneling rate Δ_x by as much as three orders of magnitude under renormalization to $T \ll T_K$ ⁵⁹ (when tunneling between the wells, the tunneling center has to drag along its screening cloud, which becomes increasingly difficult, due to the orthogonality catastrophe, at lower temperatures). Thus, the renormalized direct tunneling rate can always be assumed very small. Though this implies a large effective barrier, this does not necessarily prohibit 2CK physics, however: Zaránd and Zawadowski^{58,60} have shown 2CK physics can be obtained even if $\Delta_x = 0$, provided that the model contains some other channel for inter-well transitions, such as electron-assisted transitions via more highly excited TLS states (see appendix C 5 of II).

More serious is the assumption that the renormalized asymmetry energy Δ_r also be $\lesssim 1\text{K}$. This may seem very small when recalling that in glassy materials, the distribution $P(\Delta)$ for the asymmetry energy is rather flat, with Δ varying over many (often tens of) Kelvins. Note, though, that far from being glassy, the constrictions are believed to be rather clean (P5), containing almost perfectly crystalline Cu. Therefore, our intuition about the properties of TLSs in glasses can not be applied to the present system. For example, the TLSs could possibly be dislocation kinks. (This would naturally account for the disappearance of the ZBA when static disorder is added (P4a), since dislocation kinks can be pinned by other defects.) Since the dislocation kink would find itself in a rather crystalline material, some lattice symmetry could guarantee then that the two wells of the TLS are (nearly) degenerate and hence assure a small Δ_z and hence small Δ , etc.

Moreover, some role might be played by the mechanism of “autoselection”: This assumes that a given TLS will only be “active”, in the sense of contributing to the non-trivial V - and T -dependence of the conductance, if its (renormalized) parameters happen to be in the appropriate non-Fermi-liquid regime; if they are not, the TLS would only be an “inactive spectator” that only affects the V - and T -independent background conductance G_o . Moreover, provided that the distribution $P(\Delta_z)$ is not zero near $\Delta_z = 0$ (which seems very unlikely), there should always exist a few TLSs with $\Delta \lesssim 1\text{K}$, since Δ_x is strongly reduced by screening.

Despite the above arguments, though, the assumption that all active TLSs have $\Delta \lesssim 1\text{K}$ remains probably the weakest point in 2CK scenario. To shed more light on this matter, it would be interesting if ZBA experiments with specific type of defects with known parameters could be performed, see section X B 1.

It should be mentioned that Wingreen, Altshuler and Meir (WAM) have recently claimed¹⁵[(a)] that the 2CK interpretation is internally inconsistent if one takes into account the effect of static disorder: using values for the coupling constants deduced from the observed Kondo temperatures, they concluded that renormalized energy splitting Δ would be dramatically increased (to typical values of about 100K), and in particular that there would be zero probability for zero splitting ($P(0) = 0$). However, since their arguments neglected the physics of screening (i.e. the strong reduction of Δ_x under renormalization to lower temperatures), we believe that their conclusions, in particular that $P(0) = 0$, are not persuasive.^{15,(b), 59}. A critical discussion of their arguments is given in Appendix D of paper II.

D. Summary of Assumptions of 2CK Scenario

The 2CK interpretation of the ZBA in quenched Cu constrictions developed in this section can be summarized in the following assumptions:

- (A1) The ZBA is due to the presence in the constriction region of structural defects, namely TLSs, that interact with conduction electrons according to the non-magnetic Kondo model, which renormalizes at low energies to the non-Fermi-liquid regime of the 2CK model.
- (A2) The TLSs may occur with a distribution of (dressed or renormalized) parameters, but all “active” TLSs, i.e. those which contribute measurably to the voltage dependence of the conductance in the Cu point contacts, must have parameters which cause their behaviors to be governed by the physics of the non-Fermi-liquid fixed point of the 2CK model. This implies in particular that all of these active TLSs do not interact with each other, and have $\Delta^2/T_K < T < T_K$ for $T > 0.4\text{K}$ and $T_K > 3$ to 5K (implying $\Delta \lesssim 1\text{K}$). Other two-level systems may be present in the sample, but if their energy levels are sufficiently asymmetric (due, for instance, to the presence of static disorder) they will exhibit no Kondo effect and will contribute only to the voltage- and temperature-independent level of the background conductance.
- (A3) The number of active TLSs in a constriction can range between 1 and about 40, depending on the amplitude of the ZBA.
- (A4) The large magnetic field dependence (P8a) and the conductance transitions (P9) of the quenched Cu ZBAs are related, but not generic to the ZBA. They cannot be explained by 2CK physics alone, but involve some new energy scale on the order of V_c .
- (A5) A magnetic field does not *directly* influence the low-energy physics ($V < V_K$, $T < T_K$) of the ZBA. Therefore, 2CK physics can account for the behavior of the ZBA in quenched Cu samples at fixed H , provided that H is sufficiently small ($\lesssim 1$ T) that the conductance transitions do not influence the 2CK scaling regime (i.e. $V_c > V_K$).

VII. SCALING ANALYSIS OF $G(V, T)$

In this section, we present a detailed scaling analysis of the data and establish the scaling properties of (P6). This is a very important part of the analysis of the experiment, since the scaling properties were used above to eliminate quite a number of otherwise plausible candidate explanations of the ZBA.

Of course, the scaling properties (P6) we are about to establish are simply experimental facts, independent of any theoretical interpretation. Nevertheless, during the writing of Ref.², these properties were predicted (before their experimental verification) on the basis of the CFT solution of the 2CK model, and we shall present our analysis within this framework. We begin by giving in section VII A the general scaling argument first reported in² to motivate the scaling Ansatz for the conductance $G(V, T)$, and a back-of-the-envelope calculation of the scaling function $\mathcal{G}(x)$.

A. The Scaling Ansatz

The 2CK model is known⁹ to flow to a non-trivial, non-Fermi-liquid fixed point at $T = 0$, at which the model has been solved exactly by Affleck and Ludwig (AL), using CFT¹⁰. This fixed point governs the physics in the non-Fermi-liquid regime, namely $\Delta^2/T_K < T < T_K$ and $V < V_K$. We shall now show that the assumption of proximity to this fixed point (A2), implies the scaling properties (P6) of the conductance $G(V, T)$. This is demonstrated by a general scaling argument, and then the scaling function $\mathcal{G}(v)$ is obtained by a rough back-of-the-envelope calculation. A more careful calculation, tailored to the nanoconstriction geometry and its non-equilibrium peculiarities, is reserved for paper II.

1. General Scaling Argument

The general scaling argument leading to (P6) goes as follows²: Consider first the conductance signal $G_i(V, T)$ due to a single TLS (labeled by the index i) with $T \ll T_K^i$, $eV \ll k_B T_K^i$, $\Delta_i = 0$, but *arbitrary* ratio $eV/k_B T$. According to the general theory of critical phenomena, one expects that physical quantities will obey scaling relations in the neighborhood of any fixed point. For the conductance in the present case, a natural scaling Ansatz is:

$$G_i(V, T) = G_{io} + B_i T^\alpha, \left(\frac{A_i eV}{(k_B T)^{\alpha/\beta}} \right). \quad (12)$$

The parameters A_i and B_i are non-universal, positive constants, analogous to the a_i^\pm and b_i of Eq. (4), which may vary, for instance, as a function of the position of the TLSs within the constriction. However, the function $\mathcal{G}(v)$ should be a *universal function*, a fingerprint of the 2CK model that is the same for *any* microscopic realization thereof. It must have the asymptotic form $\mathcal{G}(v) \propto v^\beta$ as $v \rightarrow \infty$, since $G(V, T)$ must be independent of T for $eV \gg k_B T$. Due to the arbitrariness of A_i and B_i , we are free to use the normalization conventions that

$$\mathcal{G}(0) \equiv 1, \quad \mathcal{G}(v) = v^\beta + \text{constant} \quad \text{as } v^\beta \rightarrow \infty. \quad (13)$$

Now, if V is small enough, its only effect will be to create a slightly non-equilibrium electron distribution in the leads. In particular, effects that directly affect the impurity itself, like V -dependent strains, or the “polarization” of the TLS in one well due to the non-equilibrium electron distribution, etc. can then be neglected. In this case, which we shall call the *weakly non-equilibrium regime*, V only enters in the Fermi functions of the leads, in the form $[e^{\beta(\epsilon - eV/2)} + 1]^{-1}$, i.e. in the combination $eV/k_B T$, implying $\alpha = \beta$.

For a constriction with several defects, the conductance signal will be additive,⁵ i.e. (now using $\alpha = \beta$):

⁵To be more precise: the contributions of the impurities to the resistance $R = G^{-1}$ are additive, but since $R = R_o + \sum_i \delta R_i(V, T)$, with $R_o \gg \delta R_i(V, T)$, the form (14) follows.

$$G(V, T) = G_o + T^\alpha \sum_i B_i, \left(\frac{A_i eV}{k_B T} \right). \quad (14)$$

Subtracting $G(0, T)$ from this to eliminate G_o then immediately results in the scaling relation of (P6a):

$$\frac{G(V, T) - G(0, T)}{T^\alpha} = \sum_i B_i [(A_i v) - 1] \equiv F(v). \quad (15)$$

$F(v)$ is non-universal, since it depends on the A_i and B_i .

This is as far as general scaling arguments will take us; a specific theory is needed to predict α . To this end, we argue by analogy with the conductivity of a *bulk* metal containing 2CK impurities. There the bulk conductivity $\sigma(T)$ is determined, via the Kubo formula,

$$\sigma(T) = 2 \frac{e^2}{3m^2} \int \frac{d^3 p}{(2\pi)^3} [-\partial_{\varepsilon_p} f_o(\varepsilon)] \vec{p}^2 \tau(\varepsilon_p), \quad (16)$$

by the elastic scattering life-time $\tau^{-1}(\varepsilon) = -2\text{Im} \Sigma^R(\varepsilon)$, where $\varepsilon \equiv \varepsilon_p - \varepsilon_F$, and $\Sigma^R(\varepsilon)$ is the retarded electron self-energy. $\Sigma^R(\varepsilon)$ has been calculated exactly by Affleck and Ludwig, using CFT⁵⁵, for the bulk k -channel Kondo problem in the neighborhood its $T = 0$ fixed point (i.e. for $T \ll T_K$). They found that in general τ^{-1} has the following scaling form (motivated in part III, or^{55, 14, chapter 8}):

$$\tau^{-1}(\varepsilon, \{\lambda_m\}) \equiv -2\text{Im} \Sigma^R(\varepsilon, \{\lambda_m\}) = \tau_o^{-1} \left[1 + \sum_m \lambda_m T^{\alpha_m} \tilde{\tau}_m(\varepsilon/T) \right]. \quad (17)$$

The sum on m is over all perturbations to the fixed point action that one wants to consider. Each such perturbation is characterized by a non-universal parameter λ_m which measures its strength (and has dimensions of $E_m^{-\alpha_m}$, where E_m is the energy scale characterizing this perturbation), a universal scaling dimension α_m and a (dimensionless) universal scaling function $\tilde{\tau}_m(x)$. In principle all the α_m and $\tilde{\tau}_m(x)$ (but not the non-universal λ_m) can be calculated exactly from CFT, provided all the $\lambda_m T^{\alpha_m}$ are small enough that one is in the close vicinity of the fixed point. Perturbations with $\alpha_m < 0$ or > 0 are relevant or irrelevant, respectively, because they grow or decrease as the temperature is lowered at fixed λ_m . For all perturbations of interest in this paper, the scaling functions have the properties $\tilde{\tau}_m(x) = \tilde{\tau}_m(-x)$ and $\tilde{\tau}_m(x) \propto x^{\alpha_m}$ as $x \rightarrow \infty$ (the latter property follows because the perturbation must become T -independent in the limit $\varepsilon \gg T$).

AL have calculated in detail the *leading* irrelevant correction to τ_o^{-1} for the k -channel Kondo problem, for the case that no relevant perturbations are present. In other words they take $\lambda_m = 0$ for all m for which $\alpha_m < 0$, and consider only the correction corresponding to the smallest $\alpha_m > 0$, say α_1 . When referring only to this correction, we shall drop the subscript $m = 1$ and denote the corresponding parameters by $\lambda_1 \equiv \lambda$, $\alpha_1 \equiv \alpha$ and $\tilde{\tau}_1(x) \equiv \tilde{\tau}(x)$. They showed that for the k -channel Kondo problem $\alpha = \frac{2}{2+k}$, $\lambda = \tilde{\lambda} T_K^{-\alpha} > 0$ (where $\tilde{\lambda}$ is a dimensionless number of order unity) and $\tilde{\tau}(x) < 0$.⁶ (For an explicit expression for $\tilde{\tau}(x)$,

⁶The sign of λ is *a priori* undetermined in the CFT approach (see^{55, aftereq. (3.64)}); however, to conform to the expectation that the Kondo scattering rate increases as ε or T are decreased, we need $\lambda > 0$, since $\tilde{\tau}(x) < 0$.

see^{55,eq.(3.50)} or Eq. (48) of paper II).

Considering only this leading irrelevant perturbation, it follows immediately from the Kubo formula that for the 2CK problem ($k = 2$, hence $\alpha = \frac{1}{2}$), the bulk conductivity has the form

$$\sigma(T) = \sigma_o + \left(\frac{T}{T_K}\right)^{1/2} \sigma_1, \quad (18)$$

with $\sigma_1 > 0$. The unusual power law $T^{1/2}$ is a signature of the non-Fermi-liquid nature of the $T = 0$ fixed point. For a Fermi liquid, one would have had T^2 .

Although the form (17) for $\tau^{-1}(\varepsilon)$ was derived by AL only for a bulk geometry, it is natural to assume that it also governs the conductance in the nanoconstriction geometry (paper II is devoted to a careful justification of this assumption). This implies that the exponent in Eq. (12) should also be $\alpha = \frac{1}{2}$, which completes our general-principles motivation for the scaling Ansatz.

2. Back-of-the-envelope calculation of $\gamma_m(v)$

If one is willing to gloss over important subtleties, it is possible to obtain by a simple back-of-the-envelope calculation a quantitative expression for the scaling function that agrees with that found by more careful means in paper II.

Our starting point is Eq. (4), which gives the change in conductance due to back-scattering off defects in a nanoconstriction in terms of the scattering rate $\tau^{-1}(\varepsilon)$. Now, the main difference between a bulk metal and a nanoconstriction is that the latter represents a decidedly non-equilibrium situation. However, in the *weakly* non-equilibrium regime, i.e. if the voltage is small enough ($V < V_K$), it is a reasonable guess (which is substantiated in II) that the form of the scattering rate of electrons off a TLS in the nanoconstriction is not all that different as when the TLSs are in the bulk. Hence, let us boldly use⁷ the *equilibrium* form for τ^{-1} , namely Eq. (17), in Eq. (4) for ΔG , thus obtaining (to lowest order in λ_m):

$$G(V, T, \{\lambda_m\}) = G_o - e^2/h \sum_m \lambda_m T^{\alpha_m} \int d\varepsilon [-\partial_\varepsilon f_o(\varepsilon)] \sum_i b_i \frac{1}{2} [\tilde{\gamma}_m(\varepsilon - \frac{1}{2}eV a_i^+) + \tilde{\gamma}_m(\varepsilon + \frac{1}{2}eV a_i^-)] \quad (19)$$

Now write $\varepsilon/k_B T \equiv x$, $eV/k_B T \equiv v$, $f_o(v) \equiv [e^v + 1]^{-1}$, and define (universal) functions $\gamma_m(v)$ by:

$$\gamma_{b,m}(\gamma_{a,m} v) \equiv \int dx [\partial_x f_o(x)] \tilde{\gamma}_m(x + v/2). \quad (20)$$

Here $\gamma_{a,m}$ and $\gamma_{b,m}$ are universal constants, chosen such that $\gamma_m(v)$ is normalized as in Eq. (13), with $\gamma_m(\infty) > 0$:

⁷The justification for this assumption is explained in section V 2 of paper II; essentially, we assume that the leading non-equilibrium corrections to τ^{-1} are of order V/T_K , which are negligible in the weakly non-equilibrium or scaling regime.

$$, m(0) \equiv 1, \quad , m(v) = v^{\alpha_m} + \text{constant}, \quad \text{as } v^{\alpha_m} \rightarrow \infty. \quad (21)$$

Using the property $\tilde{,}_m(x) = \tilde{,}_m(-x)$ in the first term of Eq. (19), we find

$$G(V, T, \{\lambda_m\}) = G_o + e^2/h \sum_m \lambda_m T^{\alpha_m} \gamma_{b,m} \sum_i b_i \frac{1}{2} \left[, m(a_i^+ \gamma_{a,m} v) + , m(a_i^- \gamma_{a,m} v) \right]. \quad (22)$$

Let us now specialize again to the leading irrelevant perturbation, for which only $\lambda_1 \equiv \lambda \neq 0$. (Since for this case $, (x) < 0$, $\gamma_{a,1} \equiv \gamma_a$ and $\gamma_{b,1} \equiv \gamma_b$ can both be chosen positive.) In this case, Eq. (22) is precisely of the form of the scaling Ansatz Eq. (14), with $\alpha = \frac{1}{2}$. Thus we have found a “derivation” for the scaling Ansatz.⁸ Moreover, this little calculation has furnished us with an expression, namely Eq. (20), for the universal scaling function $, (v)$, in terms of the exactly known universal function $, (x)$.

This, in a nutshell, is all there is to the scaling prediction. Of course, to back up this result by a respectable calculation, considerably more care is required and several conceptual hurdles have to be overcome. These are addressed in paper II. And finally, in paper III the origin of the exponent $\alpha = \frac{1}{2}$ is explained; AL originally derived it using the full machinery of CFT, but in III it is found much more simply and directly using a recent reformulation²¹ of their theory in terms of free boson fields.

B. Scaling Analysis of Experimental Data

In this section we summarize the results of a careful scaling analysis of the experimental data², based on section 6.4.2 of¹¹, and establish that $G(V, T)$ has the properties summarized in (P6) of section IV.

1. First Test of $T^{1/2}$ and $V^{1/2}$ Behavior

As a first test of the scaling relation Eq. (14), one can consider it in the asymptotic limits $v \rightarrow 0$ and ∞ , in which the conductance becomes [using Eq. (13)]:

$$G(0, T) = G_o + T^\alpha B_\Sigma, \quad (B_\Sigma \equiv \sum_i B_i); \quad (23)$$

$$G(V, T_o) = \text{const} + v^\alpha F_o \quad \text{at fixed } T_o \ll eV/k_B \quad (F_o = \sum_i B_i A_i^\alpha). \quad (24)$$

Figs. 7(a) and 7(b) confirm that $G(0, T)$ and $G(V, 0)$ roughly conform to Eqs. (23) and (24), respectively. Values for B_Σ and F_o can be obtained from straight-line fits to these data, and are listed in table I. However, the quality of these data is not good enough to rule out other values of α , ranging from 0.25 to 0.75.

⁸Note though that Eq. (12) is actually a little too simplistic, since in Eq. (22) each defect gives rise to two terms with different a_i^+ and a_i^- . Note also that b_i, γ_o are by definition all positive constants, and $, (x) > 0$. With the choice $\lambda > 0$, discussed in footnote 6, we therefore have $G(V, T, \lambda) - G(0, T, \lambda) > 0$, consistent with experiment.

2. Scaling Collapse

A much more stringent determination of α can be obtained from the scaling properties of the combined V and T dependence of the $G(V, T)$, which, according to the 2CK interpretation, should follow Eq. (15). To check whether the data obey this relation, the left-hand side of Eq. (15) should be plotted vs. v^α . Provided that the correct value of α has been chosen, the low- T curves for a given sample should all collapse, with no further adjustment of free parameters, onto the sample-specific scaling curve $F(v)$ vs. v^α , which should be linear for large v^α [by Eq. (24)]. By adjusting α to obtain the best possible collapse, α can be determined from the data rather accurately. The 2CK scenario predicts $\alpha = \frac{1}{2}$.

The raw data for the differential conductance $G(V, T)$ of sample #1 is shown in Fig. 8(a), for T ranging from 100 mK to 5.7 K. Using $\alpha = \frac{1}{2}$, rescaling as in Eq. (15) and plotting the left-hand side vs. $v^{1/2}$, these data have the form shown in Fig. 8(b). The data at low V and low T collapse remarkably well onto one curve, which we shall call the *scaling curve*. Furthermore, $F(v)$ vs. $v^{1/2}$ has linear asymptote as $v \rightarrow \infty$, in agreement with Eq. (24).

Most of the individual curves deviate from the scaling curve for V larger than a typical scale $V_K \simeq 1meV$ (this is also roughly the voltage at which lower-lying curves in Fig. 8(a) begin to fall on top of each other). Likewise, the lowest curves in the figure, which correspond to the highest temperatures, deviate from scaling the scaling curve for almost all V . These deviations from scaling at high V and T are expected, since if either $V > V_K$ or $T > T_K$, the scaling Ansatz is expected to break down. We estimate T_K as that T for which the rescaled data already deviate from the scaling curve at $eV/k_B T \leq 1$. This gives $T_K \geq 5$ K for the defects of sample 1, which are reasonable values, as discussed in section VI C 3, and establishes the empirical relation $eV_K \simeq 2k_B T_K$.

A somewhat complimentary estimate for the highest Kondo temperatures of the TLSs in these samples comes from the temperature at which the zero-bias signals first become visible as the samples are cooled. For all 3 samples featured here, this value is approximately 10 K.

The quality of the scaling provides an exacting test of the exponent in the scaling Ansatz. Using $\alpha = 0.4$ or 0.6 instead of 0.5 in Eq. (15) produces a clear worsening of the collapse of the data (see Fig. 2(b) of²). As a quantitative measure of the quality of scaling, we define the parameter $D(\alpha)$, which is the mean square deviation from the average scaling curve $\bar{F}(v) \equiv \frac{1}{N} \sum_{n=1}^N F_n(v)$ (where n labels the different experimental curves, corresponding to different temperatures T_n), integrated over small values of $|v|$:

$$D(\alpha) \equiv \frac{1}{N} \sum_{n=1}^N \int_{-v_{max}}^{v_{max}} dv \left[F_n(v) - \bar{F}(v) \right]^2 . \quad (25)$$

$D(\alpha) = 0$ would signify perfect scaling. Taking the 5 lowest T (≤ 1.4 K) and $v_{max} = 8$ (these are the data which *a priori* would be expected to be most accurately within the scaling regime, since they are closest to the $T = 0$ fixed point), one obtains Fig. 9(a). Evidently the best scaling of the data requires $\alpha = 0.48 \pm 0.05$ [the estimated uncertainty of ± 0.05 comes from the uncertainty in the exact minimum in the curve in Fig. 9(a)]. This is in remarkably good agreement with the CFT prediction of $\alpha = \frac{1}{2}$.

We have also tested the more general scaling form of Eq. (12), and have observed scaling for $0.2 < \alpha < 0.8$, with $(\beta - 0.5) \approx (\alpha - 0.5)/2$, with best scaling for $\alpha = 0.5 \pm 0.05$. But as argued earlier on page 22, one expects $\alpha = \beta$ on general grounds.

The scaling Ansatz has also been tested on two other Cu samples. The rescaled data for sample 2 [Fig. 10(a)] collapse well onto a single curve at low V and T , for $\alpha = 0.52 \pm 0.05$ [Fig. 9(b)] and with $T_K \geq 3.5$ K. At high V and high T the non-universal conductance spikes of (P9) are visible. The data for sample #3 do not seem to collapse as well [Fig. 10(b)] (illustrating how impressively accurate by comparison the scaling is for samples #1 and #2). However, we suggest that this sample in fact displays two separate sets of scaling curves (see arrows), one for $T \leq 0.4$ K and one for 0.6 K $\leq T \leq 5$ K, with interpolating curves in between. This could be due to defects with a distribution of T_K 's, some having $T_K \simeq 0.4$ K and others having $T_K \geq 5$ K. The second (higher- T) set of curves do not collapse onto each other as well as the first, presumably because there is still some (approximately logarithmic) contribution from the $T_K \simeq 0.4$ K defects.

3. Universality

If for any sample all the A_i in Eq. (15) were equal, one could directly extract the universal scaling curve from the data. The curve obtained by plotting

$$\frac{G(V, T) - G(0, T)}{B_\Sigma T^{1/2}} \quad \text{vs.} \quad (AeV/k_B T)^{1/2}, \quad (26)$$

with A determined by the requirement that the asymptotic slope be equal to 1 [compare Eq. (13)], would be identical to the universal curve $(, (x) - 1)$ vs. $x^{1/2}$. Such plots are shown in Fig. 11(b). The fact that the scaling curves for all three samples are indistinguishable indicates that the distribution of A_i 's in each sample is quite narrow and is a measure of the universality of the observed behavior.

To make possible quantitative comparisons of the data with the CFT prediction of Eq. (20), we now proceed to extract from the data the value of a universal (sample-independent) constant [essentially a Taylor coefficient of $(, (v))$], which is independent of the possible distribution of A_i 's and B_i 's.

Consider the regime $v \gg 1$. As argued earlier, here $(, (v) \simeq v^\beta$, and since $\beta = \alpha = 1/2$, with the normalization conventions of Eq. (13) we can write, asymptotically

$$, (v) - 1 \equiv v^{1/2} + ,_1 + O(v^{-1/2}). \quad (27)$$

It follows from Eq. (15) that

$$F(v) = v^{1/2} F_0 + F_1 + O(v^{-1/2}), \quad (28)$$

where $F_0 \equiv \sum_i B_i A_i^{1/2}$ and $F_1 \equiv ,_1 B_\Sigma$. Values for F_0 and F_1 may be determined from the conductance data by plotting F versus $v^{1/2}$ and fitting the data for large $v^{1/2}$ to a straight line. For samples 1 and 2 we fit between $(eV/k_B T)^{1/2} = 2$ and 3, and for sample 3 (using only the curves below 250 mK) between 2 and 2.5.

Values for F_0 , and F_1 are listed in Table I. The uncertainties listed are standard deviations of values determined at different T within the scaling regime for each sample. From these quantities, an experimental determination of the universal number $,_1 = F_1/B_\Sigma$ can be obtained; it is listed in Table I. The values of $,_1$ are consistent among all 3 samples, in agreement with our expectation that $,_1$ should be a universal number.

Paper II will be devoted to a calculation of the universal scaling curve $\nu(v)$ and the universal number ν_1 . There it is shown that the quantitative predictions of the 2CK scenario are indeed consistent with the measured scaling curve.

C. Upper Bound on the Energy Splitting Δ

The energy splitting Δ of a TLS is a relevant perturbation to the degenerate 2CK fixed point. In the language of the magnetic Kondo problem, it acts like a local magnetic field, and hence has scaling dimension $-\frac{1}{2}$ (see (3.19) of⁶¹, or^{49,section3.4.1(e)}). Therefore a non-zero Δ implies that the electron scattering rate $\tau^{-1}(\varepsilon)$ and hence the conductance $G(V, T)$ will contain correction terms (to be labelled by $m=2$), given by Eqs. (17) and (22), respectively, with $\alpha_2 = -\frac{1}{2}$ and $\lambda_2 = \tilde{\lambda}_2 \Delta / E_2^{\frac{1}{2}}$. Here $\tilde{\lambda}_2$ is a dimensionless number of order unity, and E_2 is an energy that sets the scale at which Δ becomes important. Though this scale is not *a priori* known in AL's CFT treatment, we shall take $E_2 = T_K$, since no other obvious energy scale suggests itself.

It follows that such Δ -dependent corrections, which would spoil good V/T scaling, are unimportant only if $\lambda_2 T^{\alpha_2} < 1$, i.e. as long as

$$\Delta < (TT_K)^{\frac{1}{2}} \quad (29)$$

holds for each active TLS. Note that this inequality allows Δ to be somewhat larger than the naive estimate that would follow from $\Delta < T$. As emphasized by Zawadowski⁶², this somewhat enlarges the window of parameter space in which the 2CK scenario is applicable.

The above analysis enables us to estimate an upper bound on the energy splittings of active TLSs occurring in the quenched Cu samples. The data for samples 1 and 2 show pure $T^{1/2}$ behavior at $V = 0$ (i.e. absence of Δ -corrections) for T as small as 0.4 K. Taking $T_K \approx 5$ K, Eq. (29) implies that for any active TLS, $\Delta < 1.4$ K. This upper bound is a rather small, and was discussed at some length in section VI C 3.

VIII. RELATED EXPERIMENTS

In recent years, ZBAs have been found in a number of different nanoconstriction studies^{19,20,63}. It should be appreciated that in principle each could be caused by a different mechanism. However, here we would like to summarize a recent ZBA experiment that seems to have found a ZBA of the same type and origin as that in the quenched Cu constrictions. Keijsers, Shklyarevskii and van Kempen²⁰ studied ZBAs in mechanically controlled break junctions made from metallic glasses, which due to their disordered nature are certain to contain many TLSs. Therefore, the assumption that their ZBAs are caused by TLSs is very compelling. Since this experiment extends our general understanding of TLS-induced ZBAs, a comparison of similarities to and differences from the quenched Cu results sheds considerable further light on the latter. We review the properties of this experiment below in the form of a continuation of the list of properties compiled in section IV, together with their interpretation in terms of the 2CK scenario.

(P10) *Amplitude and Shape:*

The ZBA has qualitatively exactly the same shape and sign as that of RB's quenched Cu samples, with an amplitude of sometimes more than $100 e^2/h$. — The large amplitude is to be expected, since metallic glasses contain a high concentration of TLSs.

(P11) *Slow ZBA fluctuations:*

(a) Remarkably, in some samples the amplitude of their ZBA jumps between two (or sometimes several) values in a telegraph-noise fashion (on a time scale of seconds), evidently due to the presence of one (or sometimes several) slow fluctuators (see section VI A 1) in the constriction region.

(b) The amplitude of these telegraph-fluctuations $\delta G(V)$ is of order $1e^2/h$ or less, and depends on V . It monotonically decreases from $\delta G(0)$ to 0 as V increases from 0 to between 5 and 10 mV.

(P12) *Magnetic field:*

The ZBA shows no H -dependence. — The absence of a large H -dependence here is exactly as expected in the 2CK scenario (compare section VI C 2).

(P13) *No Conductance Transitions:* The conductance transitions (P9) that occurred in at least 80% of the quenched Cu samples have never been observed in any of the metallic-glass constrictions.

Keijsers *et al.* state that the large features of their ZBA can be explained by invoking either Zawadowski's non-magnetic Kondo model (section VI A 2) or KK's theory of TLS-population spectroscopy (section V C) to describe the interaction of electrons with the *fast* TLSs in their system. They propose that the amplitude fluctuations can be explained (in either theory) by assuming that the TLS-electron interaction strengths [V^z and V^x in Eq. (9)] are modulated between two values when the slow fluctuator hops between its two positions. This interpretation also explains why the fluctuations $\delta G(V)$ in the ZBA amplitude are largest at $V = 0$ where the ZBA is largest: with increasing V the magnitude of the ZBA-dip decreases, and hence also the magnitude of its fluctuations $\delta G(V)$ due to fluctuating interaction parameters. Conversely, the V -dependence of $\delta G(V)$ implies that the large features of the ZBA and the small amplitude fluctuations cannot be unrelated phenomena. Therefore, it is not possible, for example, to attribute the overall ZBA to a suppression in the density of states due to static disorder (analogous to the proposal of WAM for quenched Cu samples, see section V A), while assuming the additional small conductance fluctuations to be caused by an independent slow fluctuator; the problem with such a scenario would be that the amplitude of the fluctuations, though of the right magnitude of $< e^2/h$, would be V -independent.

It seems to us that the published properties of Keijsers *et al.*'s ZBA are completely compatible with Zawadowski's non-magnetic Kondo model. Note, though, that in these samples it is not necessary to assume proximity to the non-Fermi-liquid 2CK fixed point, since they did not report clear V/T scaling properties [which are in fact not to be expected for a metallic glass, because its wide distribution of Δ s violates the condition $\Delta^2 < TT_K$ of (A2)].

We do not agree, though, with the assessment of Keijsers *et al.* that their data is also fully compatible with the TLS-population spectroscopy theory of Kozub and Kulik (section V C). In this theory, ZBA's of either positive or negative sign are expected to occur [see Eq. (7)], whereas in more than 700 metallic-glass junctions Keijsers *et al.* found *only* negative anomalies for the conductance⁶⁴, consistent with VZ's theory. (The positive anomalies of their earlier experiments on Copper films are probably due to a different type of TLS than those of metallic glasses, namely dislocations¹⁹.) Note also that Kozub and Rudin's⁴⁰ mechanism for obtaining only negative anomalies within KK's theory is not applicable for metallic glasses, for which their starting assumption, namely that all bare asymmetry energies be zero, does not hold.

If the ZBAs in metallic are indeed due, as argued above, to non-magnetic Kondo physics, points (P12) and (P13) have significant implications for the interpretation of the quenched Cu constrictions: They show that both the strong magnetic field dependence (P8a) and the conductance transitions (P9) observed in the quenched Cu constrictions are *not* generic features of TLS-induced ZBAs, which lead us to suggest in section VI C 2 that these two Cu properties might be intimately related.

IX. MAGNETIC FIELD DEPENDENCE IN 2CK SCENARIO

It was stated in section VI C 2 that (contrary to our previous interpretation²) 2CK physics is unable to account for the strong magnetic field dependence (P8a) of the ZBA. To demonstrate this, we now investigate two possible mechanisms through which the 2CK scenario could produce an H -dependence for the ZBA. These are the H -tuning of the asymmetry energy $\Delta_z(H)$, and channel symmetry breaking. Both drive the system away from the degenerate 2CK fixed point (but not in precisely the same manner), so that H enters as a relevant perturbation. However, we shall conclude that both mechanisms are too weak to explain the strength of the observed H -dependence.

A. H -tuning of Δ

One possible mechanism by which H could couple to the system is by tuning^{50,51} the TLS asymmetry energy $\Delta_z(H)$, and hence the energy splitting $\Delta(H)$, which are then random functions of H (see section VI A 1). With $\Delta(H)$ as a relevant perturbation, the analysis of section VII C applies directly, and a correction to the conductance proportional to $\Delta(H)$ can be expected.

However, in this scenario, the magnetoconductance $G(H)$ should be a random function of H (since $\Delta(H)$ is), whereas it seems to be always positive for the samples investigated in more detail. Note also that it would be incorrect to attribute the non-universal non-monotonic features seen at large H for sample #2 to the random behavior of $\Delta(H)$, since closer scrutiny reveals that this behavior is due to the H -motion of the conductance transitions (P9b,v). Moreover, since H -tuning of Δ has its origin in quantum interference, it is expected to occur mainly in strongly disordered environments, which the Cu samples are decidedly not [see (P5)]. Furthermore, it causes conductance changes of order $2e^2/h$ per TLS substantially

smaller than those observed (P8a) (particularly since the signs of the conductance changes for different TLSs are random, leading to partial cancellations).

Hence, it seems as though H -tuning of Δ is not consistent with the observed H -dependence of the quenched Cu samples.

B. Channel Symmetry Breaking by H

The second mechanism by which a magnetic field could affect a 2CK system is Pauli paramagnetism, which *breaks channel symmetry* (recall that the channel index σ refers to the Pauli spin \uparrow, \downarrow) by causing a net magnetic moment $M = \mu_B^2 H N(\varepsilon_F)^{65,eq.(10.11)}$. Any such symmetry-breaking term can in principle give corrections to the critical behavior, and should hence be included in the CFT analysis.

A channel-symmetry breaking field is known to be a relevant perturbation with scaling dimension $-\frac{1}{2}$, (see eqs. (3.15) of⁶¹). Hence, in direct analogy to our analysis of the effects of Δ in section VII C, it causes a perturbation (to be denoted by $m = 3$) to the conductance $G(V, T, H)$, described by Eq. (22) with $\alpha_3 = -\frac{1}{2}$ and $\lambda_3 = \tilde{\lambda}_3 \mu_B |H| / E_3^{\frac{1}{2}}$. Here $\tilde{\lambda}_3$ is a dimensionless number of order unity, and E_3 is an energy that sets the scale at which $|H|$ becomes important. Only the absolute value of H enters, because the model is otherwise symmetric in spin \uparrow, \downarrow , so that the sign of the channel-symmetry-breaking field cannot be important.

This correction term in Eq. (22) implies that at a fixed, small temperature T_o and $V = 0$, the conductance obeys

$$G(0, T_o, H) - G(0, T_o, 0) \propto |H|. \quad (30)$$

As was argued in Ref.², the available data is at least qualitatively not in contradiction with this prediction, since Fig. 14 shows non-analyticity at $H = 0$ and an initial roughly linear behavior (P8a) (note though, that $H^{1/2}$ behavior can not be ruled out either).

What are the effects of channel-symmetry breaking at sufficiently large H ? Presumably, the polarization of the Fermi sea will become so strong that one channel of conduction electrons (the one with higher Zeeman energy) will decouple from the impurity altogether, and the system will cross over⁹ to the one-channel Kondo fixed point, at which the conductance T -exponent is $\alpha = 2$. Hence, at this fixed point the conductance, at fixed, large H , should obey the V/T scaling relation Eq. (15), with $\alpha = 2^{55,eq.(D29)}$.

However, it seems unlikely that these considerations of the large- H regime have any relevance at all for the Cu samples, since at large magnetic fields, the conductance transitions have moved into the ZBA-regime (P9b,v), presumably destroying all remnants of universal 2CK physics (Indeed, a scaling analysis of for sample #2 at fixed $H = 6$ T shows best scaling at neither $\alpha = \frac{1}{2}$ nor 2, but at $\alpha = 0.3^{31}$, though this value probably does not have special significance either.)

⁹The cross-over behavior between the fixed points [e.g. the behavior of $G(0, T, H)$] can not be calculated from CFT, which can only describe the neighborhood of fixed points; it might be possible, though, to calculate this function exactly using Bethe-Ansatz techniques.

Having investigated the phenomenology to be expected from channel symmetry breaking, let us now step back and estimate the likely magnitude of this effect. The Pauli paramagnetism that causes channel symmetry breaking merely shifts the *bottom* of the spin-up Fermi sea relative to that of the spin-down Fermi sea by $\mu_B H$, while their respective Fermi-surfaces remain aligned. Therefore, the magnitude of the effect that H has on the Kondo physics near the Fermi surface will be of order $\mu_B H/D$, where D is the bandwidth ($\sim \varepsilon_F$), and hence negligible. Though this argument is not conclusive (e.g. in poor-man scaling approaches the band-width is renormalized to much smaller values of order $D' = \max[V, T, \Delta]$), it casts serious doubts on the channel-symmetry breaking scenario, in particular because the observed amplitude of the magnetoconductance is by no means small.

Thus, we have to conclude that 2CK physics cannot account for the observed H -behavior (P8a). In section VIC2 it was therefore suggested to be linked to the H -motion of the conductance transitions [$V_c(H) \rightarrow 0$ as H increases, (P9b,v)].

X. CONCLUSIONS

A. Summary

This paper is the first in a series of three (I, II, III) devoted to 2-channel Kondo physics. We have reviewed in detail the experimental facts pertaining to a possible realization of the 2CK model, namely the non-magnetic ZBA in quenched Cu nanoconstrictions, and also integrated into our analysis insights obtained from new experiments on metallic-glass constrictions. We have summarized the facts on the Cu samples in the form of nine properties, (P1) to (P9) (section IV). Properties (P1-5), which are of a mainly qualitative nature and very robust, place very strong demands on any candidate explanations of the ZBA: the zero-bias anomalies disappear under annealing, and hence must be due to *structural* disorder; they disappear when static disorder is intentionally added, and hence cannot be due to static disorder – instead they must be due to *dynamical* impurities; they show no Zeeman splitting in a magnetic field (P8b), and hence must be of *non-magnetic* origin. These observations lead to the proposal¹ that the zero-bias anomalies are due to nearly degenerate two-level systems, interacting with conduction electrons according to the non-magnetic 2-channel Kondo model of Zawadowski⁵⁸, which renormalizes at low energies to the non-Fermi-liquid regime of the 2CK model.

We then presented a quantitative analysis of the V/T scaling behavior of the conductance $G(V, T) = G_o + T^\alpha F(eV/k_B T)$, which demonstrates unambiguously that the scaling exponent has the unusual value of $\alpha = \frac{1}{2}$, in contrast to the usual Fermi-liquid value of $\alpha = 2$. We argued that this too can naturally be understood within the phenomenology of the $T = 0$ fixed point of the 2CK model, within which the experimental verification of $\alpha = \frac{1}{2}$ constitutes the direct observation of a non-Fermi-liquid property of the system. Breakdown of scaling for larger T and V values is explained too, since for these the system is no longer fine-tuned to be close to the $T = 0$ fixed point, thus spoiling the scaling behavior. Estimates of T_K in the range 1-5 K, which is reasonable, were obtained, as well as an upper bound for the energy splitting of all active TLSs of $\Delta \lesssim k_B 1\text{K}$. This bound is rather small (and has been criticised, see section VIC3), but is enforced by the quality of the observed scaling.

The scaling analysis provides sufficiently detailed information about the low-energy physics of the system that it enabled us to rule out several other candidate mechanisms for explaining ZBAs. (An alternative interpretation of the scaling properties recently proposed by Wingreen, Altshuler and Meir can be discounted on other grounds, see section V A).

The 2CK interpretation is sufficiently successful in accounting for the observed phenomenology of the scaling properties (P6), that we believe more quantitative calculations based on this model to be justified. The remaining two papers in this series, II and III, are devoted to a quantitative calculation of the scaling function $\nu(v)$, to be compared with the experimental curve in Fig. 11(b). The final result is shown in V, Fig. 6. When our results are combined with recent numerical results of Hettler *et al.*^{12,13}, quantitative agreement with the experimental scaling curve is obtained.

The main conclusion of this investigation is therefore that *the 2CK interpretation is in qualitative and quantitative agreement with the scaling properties of the data*. It can also account for all other observed properties, with the above-mentioned two exceptions, which are apparently non-generic to the physics of TLS-induced ZBAs.

B. Open Questions and Outlook

1. Further Experiments

The magnetic field dependence of the ZBA in Cu samples is poorly understood; detailed knowledge of the conductance $G(V, H, T)$ as a function of all three arguments would be very revealing. However, as argued above, it is unlikely that the H -behavior can be understood in detail without an understanding of the conductance transitions. Nevertheless our interpretation that a magnetic field does not directly affect the low-energy physics of the ZBA can be checked by doing a V/T scaling analysis at fixed but non-zero magnetic field. If H is sufficiently small that the conductance transitions still occur at relatively high voltages (i.e. $V_c > T_K$), the scaling properties of (P6) should not be affected by having $H \neq 0$.

It would be very interesting to study the ZBA for a system for which the microscopic nature of the TLSs were better known, in order to eliminate our present lack of knowledge about their detailed parameters. An example would be the well-studied case of H interstitials tunneling in crystalline niobium^{66–68}. In this system, hydrogen molecules (which are usually mobile in Nb due to their small size) are trapped by interstitial oxygen, nitrogen or carbon, and then tunnel between two equivalent interstitial sites in the Nb crystal, resulting in a fast TLS with very well-defined parameters (e.g. the separation between the double-well minima is 1.17\AA , the tunneling rate $\Delta_o = 1.4k_B\text{K}$ and the splitting Δ has a Lorentzian distribution with a rather small characteristic width of $\bar{\Delta} = 3k_B\text{K}$). The fact that Nb has a relatively large T_c of 9.3 K should not be an insurmountable problem, since superconductivity can be suppressed by a magnetic field, which, according to (A5), should not directly affect 2CK physics.

Another possible experiment would be to study the dependence of the ZBA on the *size of the constriction*. Recently, Yanson *et al.*³⁹ have studied break junctions (point contacts with a mechanically controllable diameter, d) containing magnetic Kondo impurities. They found that as a function of decreasing d , the magnetic ZBA (due to magnetic Kondo scattering) showed a large increase in width and relative amplitude. This was interpreted as

an “enormous increase in the apparent Kondo temperature” (by more than three orders of magnitude) as d is decreased. Zaránd and Udvardi⁶⁹ have explained this effect by pointing out that a decrease of d results in a strong increase in the fluctuations in the local density of states $\delta\rho(\varepsilon, r)$, implying huge increases in $T_K = \varepsilon_F e^{-2/(3v_K\rho)}$ for some impurities. The lesson to be learned from this experiment is that since the Kondo temperature is exponentially sensitive to fluctuations in the local density of states, the occurrence of Kondo physics in a nanoconstriction necessarily leads to a strong dependence of the ZBA on constriction size. It follows that a similar experiment, with non-magnetic TLSs instead of magnetic impurities, would be very interesting: the presence or absence of a strong size effect would strongly support or conclusively rule out the 2CK interpretation, respectively. One possible problem with this proposal, though, might be that the typical Kondo temperatures need to be very small to observe a strong size effect (they were $\ll 1K$ for the magnetic impurities of³⁹), but for TLSs Kondo temperatures are known to be $\gtrsim 1K$.

2. Theoretical Questions

On the theoretical side, the 2CK model has recently been subjected to renewed scrutiny (catalyzed in part by its application to the ZBA and the claim that non-Fermi-liquid behavior has been observed). The main point of contention is whether any realistic TLS would ever flow towards the non-Fermi-liquid fixed point of the 2CK model, because of the inevitable presence of relevant perturbations that drive the system away from this point.

Wingreen, Altshuler and Meir¹⁵ have argued that static disorder could lead to a significant asymmetry energy Δ between the two states of the TLS (a relevant perturbation). We critically discuss their arguments^{15,59,(b)} in Appendix D of paper II, and judge them not to be persuasive. More recently, studying a formulation of the model that is slightly different from that introduced by Zawadowski, Fisher and Moustakas¹⁶ have discovered another relevant operator (which was then interpreted by Zawadowski *et al.*⁷⁰ to be due to particle-hole symmetry breaking). However, their conclusions have themselves been questioned in Ref.^{70,71}, where the prefactor of this new relevant operator was estimated to be negligibly small, and for other technical reasons, some of which are mentioned in appendix D of paper II.

Certainly, further theoretical work is needed to fully understand the stability, or lack thereof, of the $T = 0$ fixed point of the degenerate 2CK model. Both experimental and theoretical work would be welcome to better understand the nature of the defects giving rise to ZBAs in metal point contacts, and the parameters governing these defects. Skepticism of the 2CK interpretation of the data is not unwarranted, since this is seemingly an exotic effect. However, this model has provided a rather complete account of the experimental observations (P1-7), along with accurate predictions of the scaling properties of the conductance signals as a combined function of T and V . No other existing model, based on more familiar physics, has been able to account for the data.

Two experimental observations do appear to lie beyond the present understanding of 2CK physics: the conductance transitions (P9) and the apparently related strong magnetic field dependence (P8a). A theory of this phenomenon would be most welcome. However, these effects appear to involve either “high energy” effects or effects due to interactions between nearly degenerate TLSs which are beyond the scope of the present-day single-impurity calculations of the 2CK model, which are applicable only to the low T - and V -

regime in the neighborhood of a $T = 0$ fixed point. Since these two experimental effects are absent in metallic-glass nanoconstrictions, they should perhaps not be considered generic to the physics of TLSs in nanoconstrictions.

Acknowledgements: It is a pleasure to thank B. L. Altshuler, D. L. Cox, D. Fisher, S. Hersfield, M. Hettler, R. J. P. Keijsers, Y. Kondev, V. I. Kozub, J. Kroha, R. N. Louie, A.L. Moustakas, A. Schiller, G. Schoen, S. K. Upadhyay, G. Weiss, N. Wingreen, I. K. Yanson, G. Zaránd A. Zawadowski for discussions. This work was partially supported by the MRL Program of the National Science Foundation, Award No. DMR-9121654, and Award No. DMR-9407245 of the National Science Foundation. The research was performed in part at the Cornell Nanofabrication Facility, funded by the NSF (Grant. No. ECS-9319005), Cornell University, and industrial affiliates.

REFERENCES

- * Present Address: Institut für Theoretische Festkörperphysik, Universität Karlsruhe, D-76128 Karlsruhe, Germany
- ¹ D. C. RALPH AND R. A. BUHRMAN, Phys. Rev. Lett. **69**, 2118 (1992).
 - ² D. C. RALPH, A. W. W. LUDWIG, J. VON DELFT, AND R. A. BUHRMAN, Phys. Rev. Lett. **72**, 1064 (1994).
 - ³ D. L. COX, Phys. Rev. Lett. **59**, 1240 (1987); Physica (Amsterdam) **153-155C**, 1642 (1987); J. Magn. Magn **76 & 77**, 53 (1988).
 - ⁴ C. L. SEAMAN, M. B. MAPLE, B. W. LEE, S. GHAMATY, M. S. TORIKACHVILI, J.-S. KANG, L. Z. LIU, J. W. ALLEN AND D. L. COX, Phys. Rev. Lett. **67**, 2882 (1991).
 - ⁵ B. ANDRAKA AND A. M. TSVELIK, Phys. Rev. Lett. **67**, 2886 (1991)
 - ⁶ D. L. COX, M. JARRELL, C. JAYAPRAKASH, H. R. KRISHNA-MURTHY, AND J. DEISZ, Phys. Rev. Lett. **B62**, 2188 (1989).
 - ⁷ V. J. EMERY AND S. KIVELSON, Phys. Rev. B **46**, 10812 (1992); Phys. Rev. Lett. **71**, 3701 (1993).
 - ⁸ T. GIAMARCHI, C. M. VARMA, A. E. RUCKENSTEIN AND P. NOZIÈRES, Phys. Rev. Lett. **70**, 3967 (1993).
 - ⁹ P. NOZIÈRES AND A. BLANDIN, J. Phys. (Paris) **41**, 193 (1980).
 - ¹⁰ A. W. W. LUDWIG, Int. Jour. Mod. Phys. **B8**, 347 (1994).
 - ¹¹ D. C. RALPH, Ph.D. dissertation, Cornell University (1993).
 - ¹² M. H. HETTLER, J. KROHA, AND S. HERSHFELD, Phys. Rev. Lett. **73**, 1967 (1994).
 - ¹³ M. H. HETTLER, J. KROHA, AND S. HERSHFELD, to be published (1996).
 - ¹⁴ JAN VON DELFT, “2-Channel Kondo Scaling in Metal Nanoconstrictions – A Conformal Field Theory Calculation of Scaling Curve”, Ph.D. dissertation, Cornell University, unpublished, (1995).
 - ¹⁵ (a) N. S. WINGREEN, B. L. ALTSHULER AND Y. MEIR, Phys. Rev. Lett. **75**, 770 (1995).
(b) D. C. RALPH, A. W. W. LUDWIG, J. VON DELFT, AND R. A. BUHRMAN, Phys. Rev. Lett. **75**, 771 (1995); **75**, 2786(E) (1995).
 - ¹⁶ A. L. MOUSTAKAS AND D. S. FISHER, **53**, 4300 (1996); see also cond-mat/9607208.
 - ¹⁷ V. I. KOZUB AND I. O. KULIK, *Zh. Eksp. Teor. Fiz.*, **91**, 2243 (1986) [*Sov. Phys. JETP*, **64**, 1332 (1986)].
 - ¹⁸ V. I. KOZUB, A. M. RUDIN, AND H. R. SCHÖBER, *Solid State Com.*, **95**, 415 (1995).
 - ¹⁹ R. J. P. KEIJSERS, O. I. SHKLYAREVSKII, AND H. VAN KEMPEN, *Phys. Rev. B*, **51**, 5628 (1995).
 - ²⁰ R. J. P. KEIJSERS, O. I. SHKLYAREVSKII, AND H. VAN KEMPEN, *Phys. Rev. Lett.*, **77**, 3411 (1996).
 - ²¹ J. M. MALDACENA AND A. W. W. LUDWIG, preprint con-mat/9502109, to appear in Nucl. Phys. B, (1995).
 - ²² A. ZAWADOWSKI, Phys. Rev. Lett. **45**, 211 (1980).
 - ²³ K. VLADÁR AND A. ZAWADOWSKI, Phys. Rev. B **28**, (a) 1564; (b) 1582; (c) 1596 (1983).
 - ²⁴ P. NOZIÈRES, *J. Low. Temp. Phys.*, **17**, 31 (1974).
 - ²⁵ D. C. RALPH AND R. A. BUHRMAN, Phys. Rev. Lett. **72**, 3401 (1994).
 - ²⁶ K. S. RALLS, Ph. D. dissertation, Cornell University (1990).
 - ²⁷ A. G. M. JANSEN, A. P. VAN GELDER AND P. WYDER, J. Phys. C. **13**, 6073 (1980).
 - ²⁸ A. M. DUIF, A. G. JANSEN AND P. WYDER, J. Phys.: Cond. Matt. **1**, 3157 (1989).

- ²⁹I. K. YANSON AND O. I. SHKLYAREVSKII, Fiz. Nizk. Temp. **12**, 899 (1986) [Sov. J. Low. Temp. Phys. **12**, 509 (1986)].
- ³⁰A. A. LYSYKH, I. K. YANSON, O.I. SHKLYAREVSKII AND YU. G. NAYDYUK, Solid State Comm. **35**, 987 (1980).
- ³¹D. C. RALPH AND R. A. BUHRMAN, Phys. Rev. B **51**, 3554 (1995).
- ³²A. G. M. JANSEN, F. M. MUELLER AND P. WYDER, Science **199**, 1037 (1978).
- ³³K. S. RALLS AND R. A. BUHRMAN, Phys. Rev. Lett. **60**, 2434 (1988); Phys. Rev. B **44**, 5800 (1991).
- ³⁴K. S. RALLS, D. C. RALPH AND R. A. BUHRMAN, Phys. Rev. B **40**, 11561 (1989).
- ³⁵P. A. M. HOLWEG, J. A. KOKKEDEE, J. CARO, A. H. VERBRUGGEN, S. RADELAAR, A. G. M. JANSEN, AND P. WYDER, Phys. Rev. Lett. **67**, 2549 (1991).
- ³⁶K. S. RALLS, D. C. RALPH AND R. A. BUHRMAN, Phys. Rev. B **47**, 10509 (1993).
- ³⁷G. BERGMANN, Phys. Rep. **107**, 1 (1984).
- ³⁸P.A. LEE AND T. V. RAMAKRISHNAN, Rev. Mod. Phys. **57**, 287 (1985).
- ³⁹I. K. YANSON, V. V. FISUN, R. HESPER, A. V. KHOTKEVICH, J. M. KRANS, J. A. MYDOSH, AND J. M. VAN RUITENBEEK, Phys. Rev. Lett. **74**, 302 (1995).
- ⁴⁰V. I. KOZUB AND A. M. RUDIN, Physica B **218**, 64 (1996).
- ⁴¹Though not explicitly stated there, this suggestion follows from results contained in G. STEINEBRUNNER, *Influence of the Electromagnetic Environment on Adiabatic Quantum Transport*, Diplomthesis, Universität Karlsruhe (1994); G. STEINEBRUNNER, F. W. J. HEKKING AND GERD SCHÖN, Physica **B210**, 420 (1995).
- ⁴²J. T. MILEK, *Silicon Nitride for Microelectronic Applications*, Handbook of Electronic Materials, Vol. 3 (IFI/Plenum, 1971).
- ⁴³Y. MEIR, N. S. WINGREEN AND P. A. LEE, Phys. Rev. Lett. **70**, 2601 (1993).
- ⁴⁴L. I. GLAZMAN AND K. A. MATVEEV, Ah. Eksp. Teor. Fiz. **94**, 332 (1988) [Sov. Phys. JETP **67**, 1276 (1988)]; Pis'ma Zh. Eksp. Teor. Fiz. **48**, 403 (1988) [JETP Lett. **48**, 445 (1988)].
- ⁴⁵Y. XU, A. MATSUDA, AND M. R. BEASLY, Phys. Rev. **B 42**, 1492 (1990); D. EPHRON, Y. XU AND M. R. BEASLEY, Phys. Rev. Lett. **69**, 3112 (1992).
- ⁴⁶D. V. AVERIN AND K. K. LIKHAREV, in *Mesoscopic Phenomena in Solids*, ed. B. L. ALTSHULER, P. A. LEE AND R. A. WEBB, Elsevier, (1991), Ch. 6.
- ⁴⁷J. KÖNIG, J. SCHMIDT, H. SCHOELLER AND G. SCHÖN, Czech. J. Phys. **46 S 4**, 2399 (1996); preprint cond-mat/9608081, to be published in Phys. Rev. B. (1996).
- ⁴⁸P. W. ANDERSON, B. I. HALPERIN AND C. M. VARMA, Philos. Mag. **25**, 1 (1972); W. A. Phillips, J. Low Temp. Phys. **7**, 351 (1972).
- ⁴⁹D. L. COX AND A. ZAWADOWSKI, Review Article: "Exotic Kondo Effects in Real Materials", to be published (1995).
- ⁵⁰N. W. ZIMMERMAN, B. GOLDING, W. H. HAEMMERLE, Phys. Rev. Lett. **67**, 1322 (1991).
- ⁵¹G. GOLDING, N. M. ZIMMERMAN, S. N. COPPERSMITH, Phys. Rev. Lett. **68**, 998 (1992).
- ⁵²B. L. AL'TSHULER AND B. Z. SPIVAK, Pis'ma Zh. Eksp. Teor. Fiz. **49** 671 (1989) [JETP Lett. **49**, 772 (1989)].
- ⁵³A. ZAWADOWSKI AND K. VLADÁR, in *Quantum Tunneling in Condensed Media*, ed. YU. KAGAN AND A. J. LEGGETT (Elsevier, 1992) p. 427.

- ⁵⁴ A. MURAMATSU AND F. GUINEA, Phys. Rev. Lett. **57**, 2337 (1986).
- ⁵⁵ I. AFFLECK AND A. W. W. LUDWIG, Phys. Rev. **B48**, 7297 (1993).
- ⁵⁶ A. C. HEWSON, *The Kondo Problem to Heavy Fermions*, Cambridge University Press, 1993.
- ⁵⁷ K. VLADÁR, A. ZAWADOWSKI AND G. T. ZIMÁNYI, Phys. Rev. B **37**, 2001, 2015 (1988).
- ⁵⁸ G. ZARÁND AND A. ZAWADOWSKI, Phys. Rev. Lett. **72**, 542 (1994).
- ⁵⁹ G. ZARÁND AND A. ZAWADOWSKI, Physica B 218, 60 (1996).
- ⁶⁰ G. ZARÁND AND A. ZAWADOWSKI, Phys. Rev. B **50**, 932 (1994).
- ⁶¹ I. AFFLECK, A. W. W. LUDWIG, H.-B. PANG AND D. L. COX, Phys. Rev. **B45**, 7918 (1992).
- ⁶² We thank A. ZAWADOWSKI for pointing out this argument to us.
- ⁶³ A. I. AKIMENKO AND V. A. GUDIMENKO, Solid State Comm. **87**, 925 (1993).
- ⁶⁴ R. J. P. KEIJERS, private communication.
- ⁶⁵ J. M. ZIMAN, *Principles of the Theory of Solids*, 2nd Ed., Cambridge University Press (1972).
- ⁶⁶ W. MORR, A. MÜLLER, G. WEISS, H. WIPF AND B. GOLDING, Phys. Rev. Lett. **63**, 2084 (1989).
- ⁶⁷ H. GRABERT AND H. WIPF, Adv. Solid State Phys., **10**, 1 (1990).
- ⁶⁸ We thank G. WEISS for drawing our attention to the Hydrogen in Niobium tunneling system.
- ⁶⁹ G. ZARÁND AND L. UDVARDI, Phys. Rev. B, **54**, 7606 (1996).
- ⁷⁰ A. ZAWADOWSKI AND G. ZARÁND, preprint (1996).
- ⁷¹ J. YE, preprint cond-mat/9609076 (1996).

FIGURES

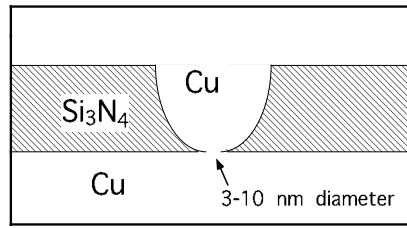


FIG. 1. Cross-sectional schematic of a metal nanoconstriction. The hole at the lower edge of the Si₃N₄ is so small that this region completely dominates the resistance of the device.

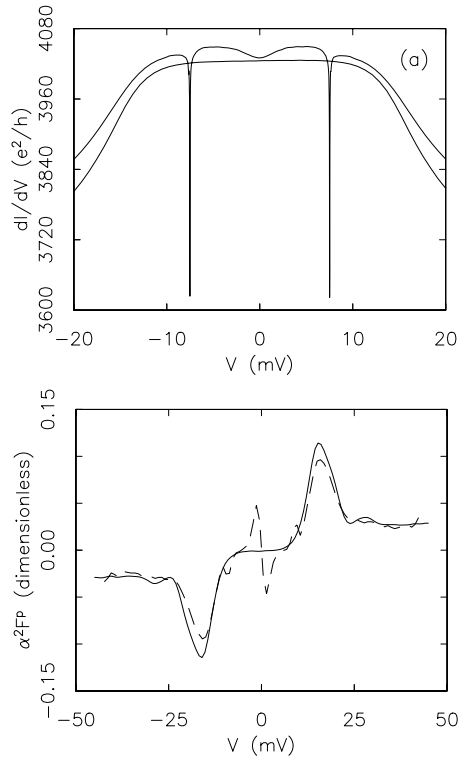


FIG. 2. A typical conductance curve for a constriction containing structural defects: (a) The upper curve, showing a dip in conductance at $V = 0$ and voltage-symmetric spikes, is the differential conductance for an unannealed Cu sample at 4.2 K. The lower curve shows the conductance of the same device at 4.2 K, after annealing at room temperature for 2 days. The curves are not artificially offset; annealing changes the overall conductance of the device by less than 0.5%. (b) Point contact phonon spectrum at 2 K for the device before anneal (dashed line) and after anneal (solid line).

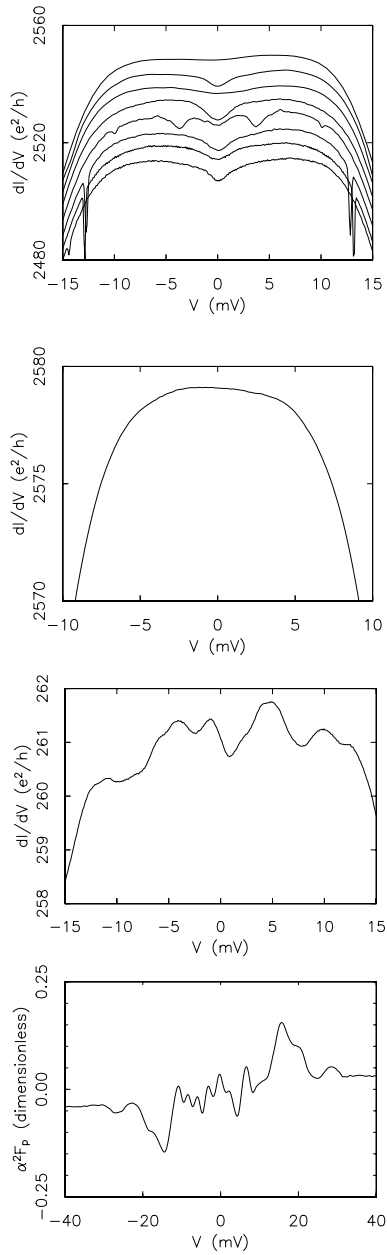


FIG. 3. (a) Differential conductance versus voltage at 4.2 K for a Cu sample which underwent repeated thermal cycling¹¹. The time sequence runs from the bottom curve to the top. Curves are artificially offset. The first 2 excursions were to 77 K, the next 5 to room temperature. (b) Differential conductance for a Cu sample intentionally doped with 6 % Au. Static impurities reduce the electronic mean free path but completely eliminate the zero-bias anomaly of interest to us. (c) Differential conductance and (d) point contact spectrum for a Cu device at 1.8 K in which disorder has been created by electromigration (which means that a high bias (100-500 mV) has been applied at low temperatures so that Cu atoms moved around).

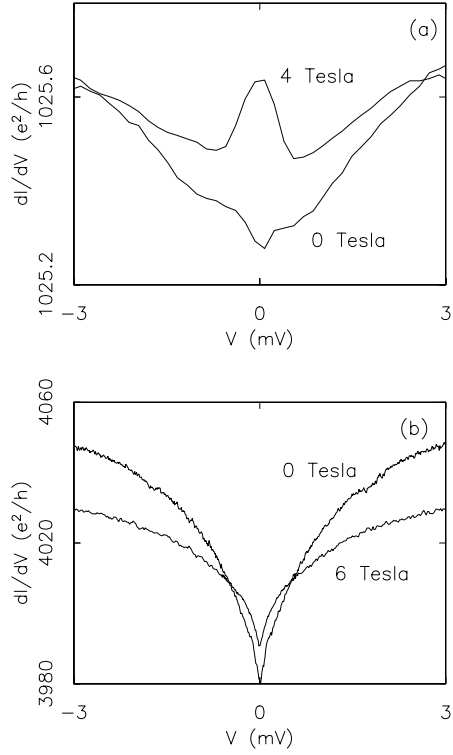


FIG. 4. (a) Conductance signals for 500 ppm magnetic Mn impurities in Cu at 100 mK, showing Zeeman splitting in an applied magnetic field. (b) The ZBA signals from quenched Cu samples exhibit no Zeeman splitting, demonstrating that they are not due to a magnetic impurity. However, the shape and amplitude of the ZBA does depend on magnetic field.

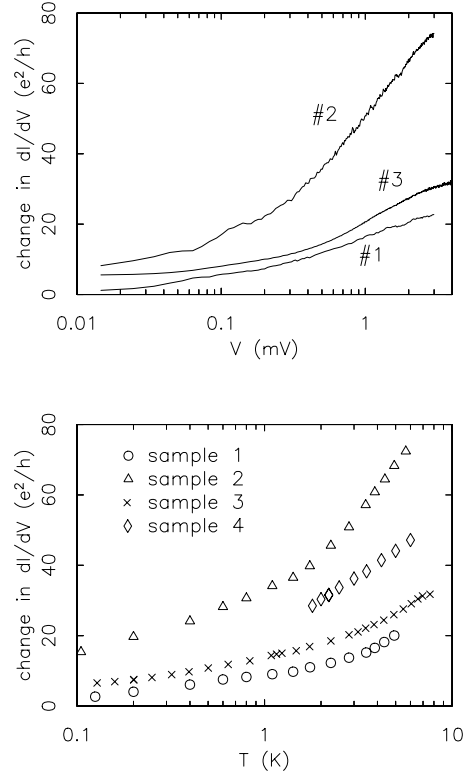


FIG. 5. (a) V -dependence of the differential conductance for $B = 0$ and $T = 100$ mK. (b) T -dependence of the conductance for $B = 0$ and $V = 0$. Straight lines illustrate regions of logarithmic V - and T -dependencies.

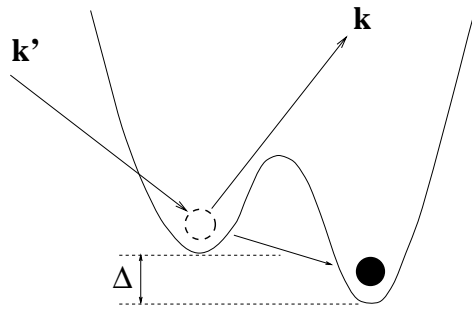


FIG. 6. A generic two-level-system, with (bare) energy asymmetry Δ and tunneling rate Δ_0 . An electron-assisted tunneling event is depicted: an electron scatters of the TLS and induces the atom to tunnel.

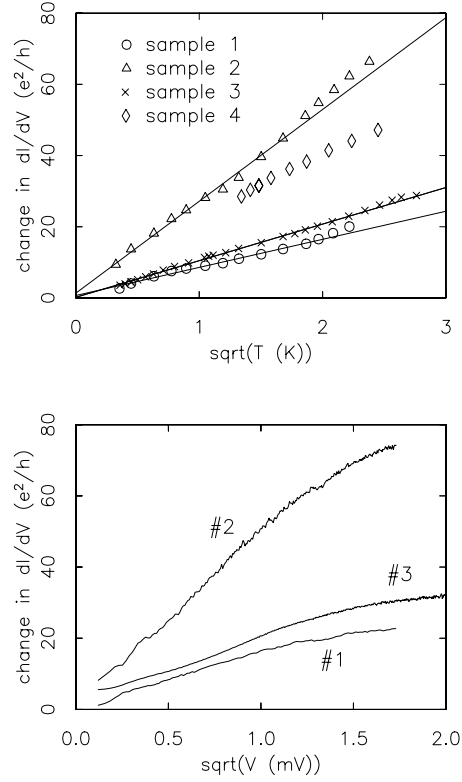


FIG. 7. (a) Temperature dependence of the $V = 0$ conductance $[G(0, T) - G(0, T_0)]$ for 4 unannealed Cu samples, plotted versus $T^{1/2}$. The values of $G(0, T)$ for the different samples, extrapolated to $T = 0$ as shown are for sample #1: $2829 e^2/h$, sample #2: $3973 e^2/h$, sample #3: $30.8 e^2/h$, and sample #4: approximately $2810 e^2/h$. (b) Voltage dependence of the differential conductance at $T = 100$ mK for some of the same samples as in (a), plotted versus $V^{1/2}$. The size of deviations from $T^{1/2}$ behavior in (a) (1 part in 3000) is consistent with the magnitude of amplifier drift in these measurements, as they were performed over several days. The V -dependent measurements in (b) are less subjective to such drift problems, as they are taken over a much shorter time span.

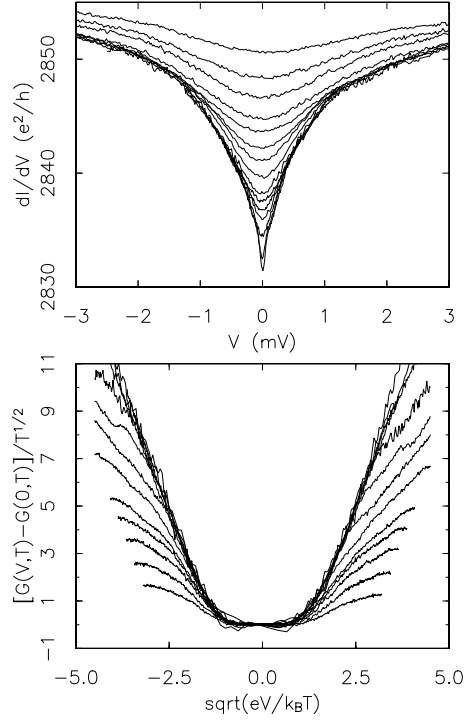


FIG. 8. (a) Voltage dependence of the differential conductance for sample #1 of 7, plotted for temperatures ranging from 100 mK (bottom curve) to 5.7 K (top curve). (b) The same data, rescaled according to Eq. (15) with $\alpha = \frac{1}{2}$, and plotted vs. $v^{1/2} = (eV/k_B T)^{1/2}$. The low-temperature, low-voltage data collapse onto a single curve [linear for large $v^{1/2}$, in agreement with Eq. (24)], with deviations when the voltage exceeds 1 mV.

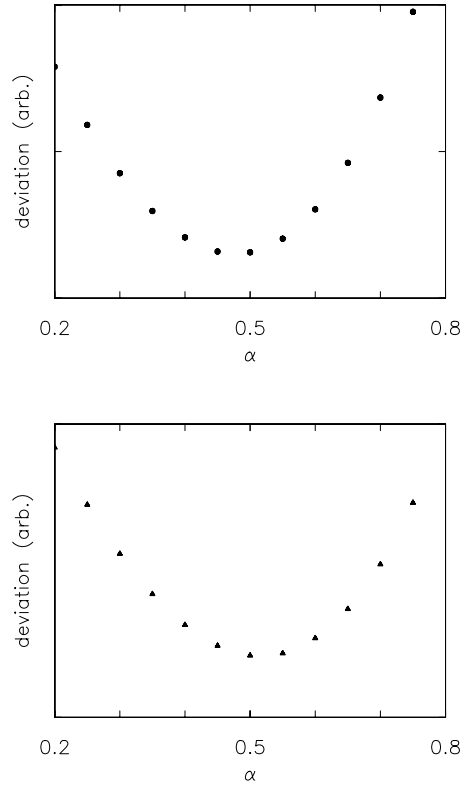


FIG. 9. The deviation parameter $D(\alpha)$ of Eq. (25), which quantifies the quality of scaling, for (a) sample #1 and (b) sample #2. The minimum of $D(\alpha)$ defines the value of α that gives the best scaling, giving $\alpha = 0.48 \pm 0.05$ for sample #1 and $\alpha = 0.52 \pm 0.05$ for sample #2.

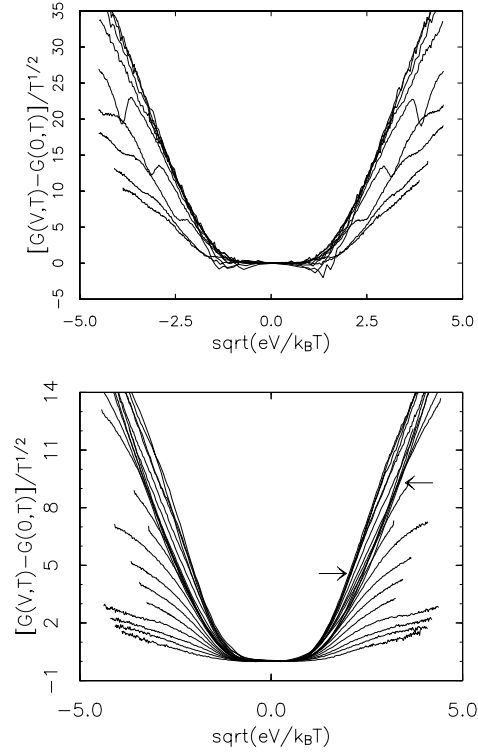


FIG. 10. (a) Differential conductance data for sample #2, at temperatures from 200 mK to 5.7 K, and (b) for sample #3, at temperatures from 50 mK to 7.6 K, rescaled according to Eq. (15) and plotted vs. $v^{1/2} = (eV/k_B T)^{1/2}$. The low-voltage, low-temperature data collapse well onto one curve for sample #2, but not for sample #3, partly due to the existence of TLSs with Kondo temperatures within in (rather than above) the temperature range of the measurement.

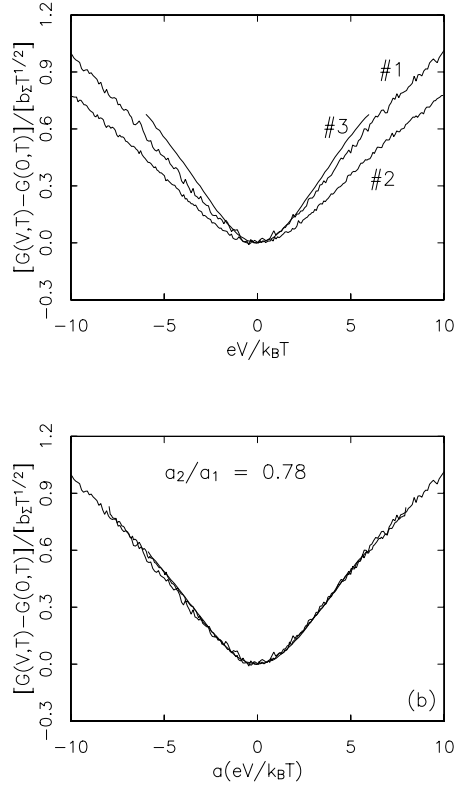


FIG. 11. Representative conductance curves which lie along the scaling curves for samples # 1, 2 and 3 of each of the three samples in Figs. 8(b), Fig. 10(a) and (b), respectively. For sample #1, the curve corresponds to $T=1.1$ K, for sample #2 1.4 K, and for sample #3 250 mK. The reason for selecting these particular curves was that among all those lying along the scaling curve, they had the best signal-to-noise ratio for each sample. (a) The y -axis is scaled by the value of B_S determined from the temperature dependence of the $V = 0$ conductance for each sample (values listed in Table 6.1). (b) In addition, the x -axis is scaled with a number a_i for each sample. The scaling curves for all three samples seem to lie on one universal curve.

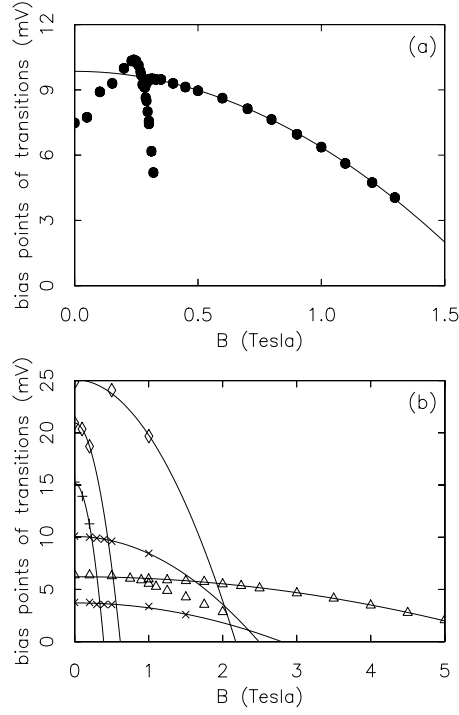


FIG. 12. (a) Transition voltage $V_c(H)$ of the conductance transition³¹ as a function of magnetic field for a quenched Cu constriction at 4.2 K, showing bifurcation (P9b,iv). At high fields $V_c(H) \rightarrow 0$ (P9b,v), the dependence on H being quadratic. (b) $V_c(H)$ for five other samples at 4.2 K, with associated decreases to 0, quadratically in H .

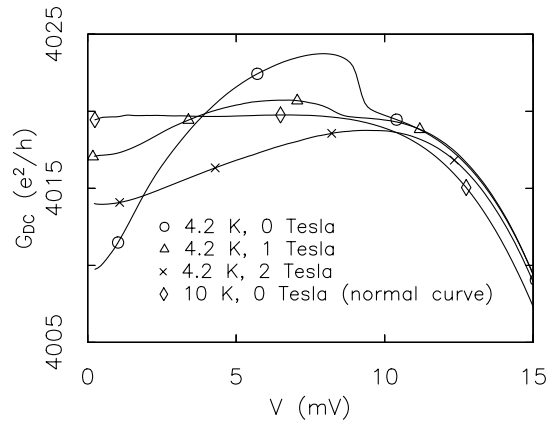


FIG. 13. The *DC* conductance G_{DC} (as opposed to differential conductance G used in all other plots) at several magnetic fields for a quenched Cu sample³¹. An increasing magnetic field broadens the conductance transition at V_c and moves V_c toward zero voltage, destroying the enhancement at $V = V_c$ of G_{DC} above the normal conductance. Note that although a large applied magnetic field eliminates the conductance transition, a $V = 0$ minimum in the conductance remains.

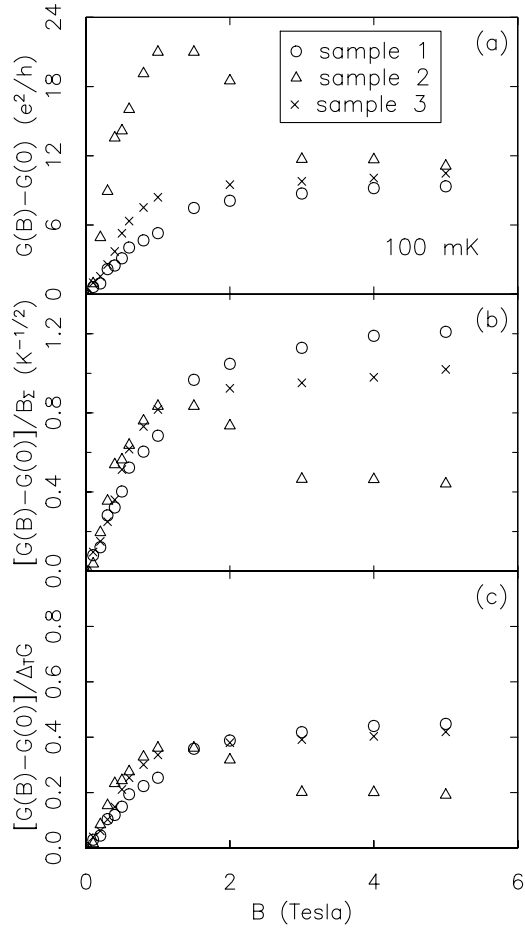


FIG. 14. Magnetic field dependence of the $V=0$ conductance for the 3 unannealed Cu samples at 100 mK. (a) Absolute magnetoconductance. (b) Magnetoconductance scaled by the value of B_z for each sample. (c) Magnetoconductance relative to the change in conductance between 100 mK and 6 K. An applied magnetic field alters, but does not eliminate, the zero-bias conductance signal due to TLSs.

TABLES

TABLE I. Measured parameters of the scaling functions for the Kondo signals in 3 Cu samples. B_Σ , F_0 and F_1 have units $K^{-1}e^2/h$, and β_1 is dimensionless.

#	B_Σ	F_0	F_1	$\beta_1 = \frac{F_1}{B_\Sigma}$
1	7.8 ± 0.2	4.2 ± 0.3	-5.7 ± 0.9	-0.73 ± 0.11
2	25.2 ± 0.7	12.8 ± 0.8	-19.7 ± 1.5	-0.78 ± 0.06
3	10.3 ± 0.4	6.0 ± 0.6	-7.7 ± 1.6	-0.75 ± 0.16